NASW-4435

IN-18-CR
73901
P-100

NASA/USRA

ADVANCED DESIGN PROGRAM

OLD DOMINION UNIVERSITY

1990-1991

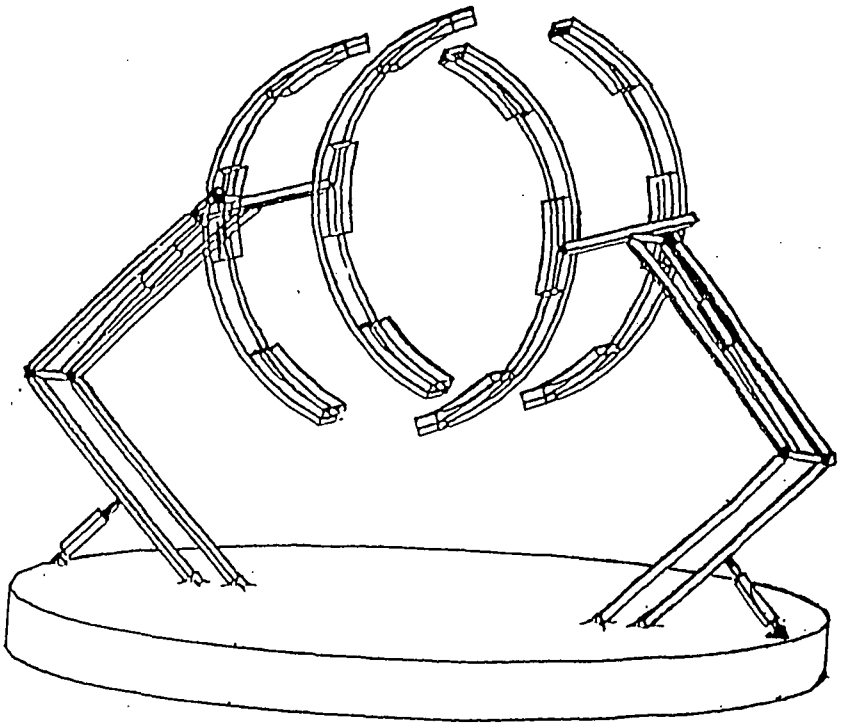

CONCEPTUAL DESIGN OF AN ORBITAL DEBRIS COLLECTOR

(NASA-CR-189989) CONCEPTUAL DESIGN OF AN ORBITAL DEBRIS COLLECTOR (Old Dominion Univ.) 100 p CSCL 22B

N92-21242

Unclas
G3/18 0073901

ABSTRACT

The current Lower Earth Orbit (LEO) environment has become overly crowded with space debris. It is necessary to provide an effective means of removing debris potentially hazardous to operating satellites and manned missions. An evaluation of types of debris is presented in order to determine which debris poses the greatest threat to operations in space, and would therefore provide a feasible target for removal. A target meeting these functional requirements was found in the Cosmos C-1B Rocket Body. These launchers are spent space transporters which constitute a very grave risk of collision and fragmentation in LEO. The motion and physical characteristics of these rocket bodies have determined the most feasible method for removal. The proposed Orbital Debris Collector (ODC) device is designed to attach to the Orbital Maneuvering Vehicle (OMV), which provides all propulsion, tracking and power systems. The OMV/ODC combination, the Rocket Body Retrieval Vehicle (RBRV), will match orbits with the rocket body, use a spin table to match the rotational motion of the debris, capture it, despin the debris, and remove it from orbit by allowing it to fall into the earth's atmosphere. A disposal analysis will be presented to show how the debris will be deorbited into the earth's atmosphere. In order to fully illustrate the conceptual means of operation a sample mission is then described. A rough physical model was built to illustrate the basic procedure of capture. Conclusions are drawn, and future recommendations for further research are given.

ACKNOWLEDGEMENTS

The Orbital Debris Collector is a project in which six senior mechanical engineering students at Old Dominion University participated. Their accomplishments and the support of USRA should be noted.

Dr. Robert L. Ash	Department Chairman and USRA project advisor
Dr. J. Phillip Raney	Orbital Debris Collector faculty advisor
Peter O'Donoghue	Editor of this report

ORBITAL DEBRIS COLLECTOR TEAM

Peter O'Donoghue **Project Manager**

Brian Brenton **Asst. Project Manager**

Ernest Chambers
Thomas Schwind
Christopher Swanhart
Thomas Williams

Table of Contents

Acronyms i
1. Background 1
2. Introduction 9
3. Target Selection 12
    1. Initial Target Guidelines 12
    2. Target Type Selection 13
4. Rotational Motion Analysis 18
5. Evolution of Design 22
6. Conceptual Design 29
    1. Spin Table and Associated Equipment 29
    2. Brakes 30
    3. Arms 36
    4. Mechanisms of Arms 37
    5. Camera Location 40
    6. Thermal Protection 41
    7. Concepts for Improving Lifecycle Performance 43
7. Disposal Analysis 45
    1. Translation Motion Analysis 45
    2. Delta V Analysis 46
    3. Important Atmospheric Reentry Relationships 50
    4. Skipback Phenomenon 53
8. Sample Mission 55
    1. Deployment 55
    2. Initial Approach 56
    3. Proximity Analysis 57
    4. Capture 58
    5. Despin and Release 58
9. Physical Model 60
10. Conclusions/Future Directions 62
References 63
Appendices 67

ACRONYMS

C-1B	Soviet Low Earth Orbit Rocket System
EVA	Extravehicular Activity
LEO	Lower Earth Orbit
NASA	National Aeronautics and Space Administration
NMI	Nautical Miles
NORAD	North American Aerospace Defense Command
ODC	Orbital Debris Collector
OMV	Orbital Maneuvering Vehicle
RAE	Royal Aircraft Establishment
RBRV	Rocket Body Retrieval Vehicle
RMS	Remote Manipulator System
RPS	Revolutions Per Second
TSR	Tumbling Satellite Retrieval (Kit)
USRA	Universities Space Research Association

1. BACKGROUND

Orbiting Debris has become a severe problem in the recent years. Man made debris has reached surprising levels. The current tracking and cataloguing system can detect only relatively large debris. This is a small percentage of the objects that can cause significant damage to spacecraft. A better understanding of what orbital debris consists of, how it was formed, and it's location is needed if we are to understand the potential hazards, and continue our advance into space.

With the launch of Sputnik I in 1957, the man-made orbital environment was created. By the end of the 1960s, total launches reached an average rate of 127 missions per year, and have remained at this approximate level ever since [Ref. 1]. This high rate of continuous launches has, over a period of decades, resulted in a glut of dysfunctional satellites and debris in orbit.

The population of objects in LEO is currently monitored by the North American Aerospace Defense Command (NORAD) which catalogs and determines trajectories and decay rates for all objects picked up by its ground-based radar systems. Currently, NORAD is capable of tracking only those objects greater than 4 to 10 cm in diameter. Figure 1.1 shows a computer generated image of the earth's artificial satellite population. Future projections based on these catalogued

objects show a dangerously crowded earth orbit.

Propellant explosions, one of the major causes of debris, can have one of several causes. The two current theories are that either solar radiation causes the propellant tanks to over-pressurize, or that collision with other debris causes the rocket body to explosively fragment due to internal pressure. Venting the rocket body tanks should largely eliminate this breakup. Research into Hypervelocity impacts show that an unpressurized upper-stage tank remains mostly intact following impact, while a pressurized container is ruptured into several large pieces, and numerous smaller fragments. The conclusions to this experimental research state that unless the stage is vented, the pressure "can lead to catastrophic destruction by an object of relatively small mass hitting at speeds greater than 4 km/sec". This value of 4 km/sec is relatively slow for the average estimated collision velocity of orbital debris. Typical of these explosions is that of the Spot 1 Ariane Third Stage, which broke up into almost 500 detectable pieces [Ref. 2].

There is evidence that there have been other breakups in third-stage tanks, and there are many rockets still in LEO that were placed there before it became standard practice to provide a method of post-operational venting.

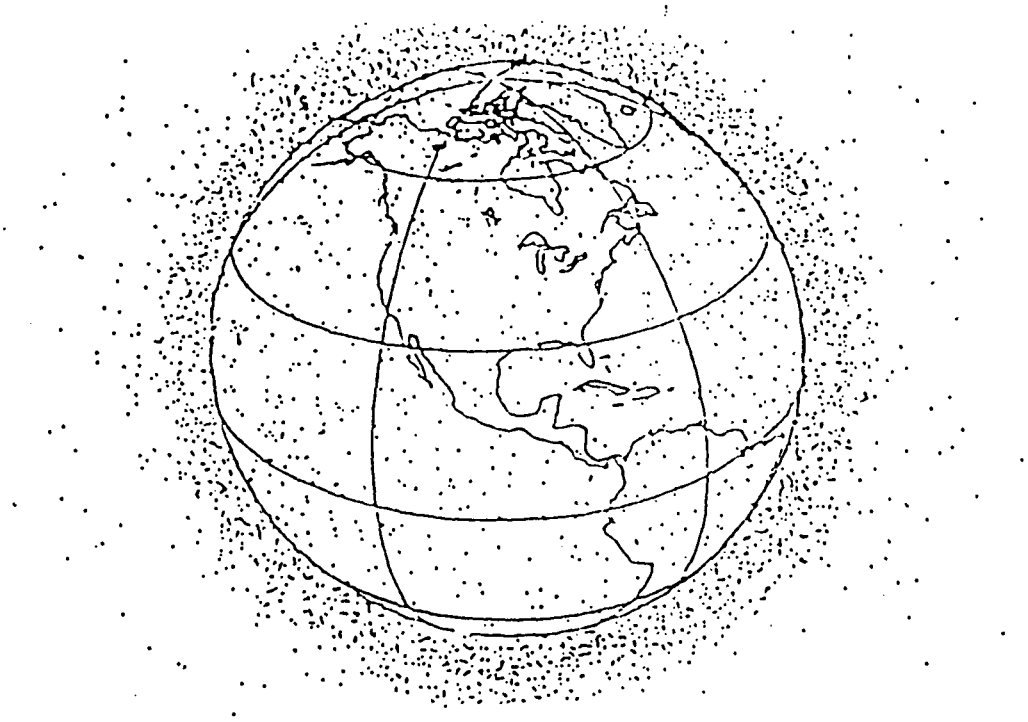

Figure 1.1 - A NASA Computer Projection Based on NORAD Data

Dr. Donald Kessler, the NASA Johnson Space Center expert on orbital debris, states that "a large number of satellite breakups still occur and with time, collisions will cause a rising fraction of breakups in space" [Ref. 3]. It is evident that these rocket bodies must be removed from orbit before they fragment and contribute hundred-fold increases to the orbital debris population.

At this time, it is accepted that the level of orbital debris is not yet prohibitive for spacecraft. However, this could easily change. A large effort has gone into determining the future numbers and types of orbital debris. Even if no

more launches were made, the level of orbital debris is expected to continue to grow due to continuing collisions generating more fragments.

Extensive computer modeling allowed a group of scientists from the Technical University Braunschweig [Ref. 4] to develop the future orbit projections. Figure 1.2 shows the number of expected collisions expected for various launch growth-rate models. They determined that after 20 years, the number of trackable objects in near earth orbit will increase from 7000 to 18000, and again after 45 years to 33000. The satellites in the higher orbits take centuries to decay. Their report states that "this higher altitude is most sensitive to a permanent pollution with man-made objects ." Furthermore, as these satellites decay, they decay through the orbits most frequently used. It is clear we must take action now to prevent further danger to our future space environment.

The average velocity of impact is 10 km/sec [Ref. 5]. At this velocity a chip of paint would puncture a standard space suit. In 1983 a fleck of paint left a 4 mm gouge in the windshield of the Space Shuttle *Challenger*. The paint fleck was estimated by NASA to be 0.2 mm in diameter and travelling at 3 to 6 km/sec. Although this was a relatively minor incident, they might not have been so fortunate. The object could have been much larger. Considering there are many thousands of objects of this small size and density travelling at unknown

trajectories in similar orbits, this poses grave dangers to any space mission.

The danger of an impact is only relative to the likelihood of its occurrence. The risk of collision between an active satellite and orbiting debris becomes greater everyday. In a period of two weeks, five military and one government satellites were involved in near collisions in 1988. These satellites were saved by moving the active satellites out the path of the tracked debris [Ref. 6]. Most satellites, such as the Hubble Telescope, cannot be moved. Should an impending collision be detected, Mission Control could only wait for the probably catastrophic[1] collision. It is clear that orbital debris poses a significant threat to our space missions. We must determine how to prevent this from affecting our objectives in space.

Scientists' greatest concern, is a chain reaction of satellite impacts. An impact between a fragment and a major object such as a spent fuel tank, would likely produce hundreds of fragments (as seen in the Ariane third stage analysis). These fragments could then collide with other debris to produce even more fragments in a geometrical progression. Donald Kessler predicts "the ultimate hazard of satellite-breakup debris is collision with larger space objects and the

---

[1] A catastrophic event is considered to be complete destruction of the object, and the generation of new fragments which can cause equally destructive collisions.

subsequent creation of great numbers of secondary debris". It is predicted that the likelihood of a catastrophic event is 3.7 percent [Ref. 7]. Should this occur, there would be a belt of orbiting debris circling the earth that would destroy anything launched into it for centuries. It is necessary to understand and deal with this problem immediately. Even without the total destruction of our space environment, the risk of space collisions will become more probable, making any space venture costly both in resources and potentially in human lives.

There are many things that can be done to alleviate the hazard of space debris. These can generally be broken down into two categories: things that can prevent future debris, and things which can help eliminate existing debris.

The following is a list developed by Donald Kessler, and imparts what we now know to conduct future efforts without contributing to debris:

> 1) "Satellites should remain "intact" until re-entry. This would require that both payloads and rockets be designed to minimize the possibility of on-orbit explosions and that they retain structural integrity and intact thermal surfaces.
>
> 2) Population growth should be monitored for debris sizes smaller than those currently detected on the ground. This would not only provide a check for model predictions but would also detect any sources and provide sufficient data either to eliminate the sources or to design shields to protect spacecraft from the measured environment.

> 3) Rocket stages used to transfer payloads from low earth orbit to geosynchronous orbit should be re-entered within a year. When planned, the stages could easily be re-entered. Otherwise, they could remain in orbit for a very long time and pose a hazard to satellites in both low earth orbit and geosynchronous orbit.
>
> 4) Any program that plans to place either large structures or a large number of objects in Earth orbit should be carefully examined for orbital-debris implications. Such programs, if not carefully conceived, could initiate a fragmentation process that could cascade to other satellites."

These guidelines should be strictly followed by all launching nations. If this can be achieved, there will be an eventual decline of objects in LEO.

The other tactic involves the elimination of present debris. One important means might be to slow down clouds of small orbital debris from previous breakups so they decline rapidly into the Earth's atmosphere. Another important action would be to remove large debris such as spent rockets from orbit using an Orbital Debris Collector (ODC) attached to the previously designed Orbital Maneuvering Vehicle (OMV). This ODC/OMV combination would remove large structures before they can be fragmented, thereby reducing the chance of further fragmentation.

It is a combination of both these tactics on a worldwide scale that must immediately be implemented if we are to continue to make use of and explore

space. The only way to achieve the removal of large quantities of debris is through attrition. We must learn what is up there and how to protect ourselves while we wait for it to slowly be drawn into Earth's atmosphere.

2. INTRODUCTION

Having consulted past work on this subject, a decision was made to target larger articles of debris for two major reasons. The first of these was the ease of capture. It is conceivably easier to catch and control larger bodies. The second was that although micro-fragments provide the most serious threat to operational satellites in space, larger bodies could be viewed as potentially billions of post collision micro-fragments. Therefore action should be taken to remove the larger debris before it can fragment.

Having researched the extent of the problem of debris in LEO, it was decided to select discrete regions of space which are more adversely affected by the potential of collisions with orbital debris. Efforts were made to cluster debris into like categories in these areas. The exact region that was analyzed was the region of LEO of altitudes between 700 and 1000 km and angles of inclination between 70 and 85 degrees. This is the most potentially hazardous region of space. When discussing this project with Dr. Donald Kessler [Ref. 8], he suggested attempting to design a device to remove debris from this region, and stressed the urgency and real potential of the occurrence of disastrous collisions in this region, should there be no debris removal soon. He described this region

as "collisionally unstable", implying the probability of a cascading effect of collisions in this region as a result of one single impact. Research into exactly what debris constituted the most feasible target for the RBRV, was a key element of this project.

The second part of the extensive literature search comprised of an in-depth analysis of previous research into the removal of debris from LEO. The University of Arizona Autonomous Space Processor for Orbital Debris Universities Space Research Association (USRA) Team [Ref. 9] provided an excellent basis from which to attack the problem of orbital debris. Their main progress was in the design and the development of a prototype solar cutter to be used in conjunction with some predetermined means of capturing debris. The University of Texas' USRA team [Ref. 10], was also an excellent source of information especially in the areas of different means of capturing debris and their in-depth astrodynamic analyses.

One of the major decisions made in the progress of the ODC team was that of the assumption of use of the OMV as a base vehicle for the ODC kit. This decision was justified primarily on the basis of work by Petro [Ref. 11] and on two OMV user reports [Refs. 12,13]. The most interesting envisaged function of the OMV was the capture of satellites for maintenance purposes with utilizing a

Tumbling Satellite Recovery Kit (TSR). The information on the TSR kits was graciously provided by Dr. James Turner of NASA Marshall Space Flight Center, and came in the form of a series of reports by Grumman Aerospace [Refs. 14,15,16] and Martin Marietta [Ref. 17]. The Grumman Aerospace reports show conclusively that the capture of a spinning satellite is feasible. Extensive simulations have been run by Grumman Aerospace in their large Amplitude Space Simulator to prove that this is a practical solution.

These reports formed the basis of the ODC design, especially the use of the spin table to match the rotational motion of a body in space. Invaluable information was provided by the Grumman reports, especially in the documents pertaining to the testing of the prototype, and in the areas of cameras and lighting. However, the functional requirement of the TSR kit was to retrieve bodies rotating in a spinning motion about the longitudinal axis of the body, which differs from the diametral rotation of spent rocket bodies. The concept of using a spin table assembly to match rotational motion of the payload mounted on the OMV is a direct result of the Grumman reports. However, totally new designs on the arms and cradles are provided as are details of thermal shielding, material selection, and mechanisms analyses.

3. TARGET SELECTION

3.1. INITIAL TARGETS GUIDELINES

Examination of the Satellite Situation Report [Ref. 18] published by Goddard Space Flight Center and The R.A.E. (Royal Aircraft Establishment) Table of Earth Satellites 1957-1986 [Ref. 19], provided the starting point for the ODC target determination process. Using Dr. Donald Kessler's suggestions as baseline acceptance criteria [Ref. 8], it was possible to narrow the list of possible targets considerably. The initial acceptance criteria would consider only Soviet satellites in the 70 to 85 degree angles of inclination and from 700-1000 km at apogee.

These criteria make for a realistic design goal because the first generation of orbital clean-up vehicles will have to focus on the already over-congested LEO regions. Because of orbital precession and other forces, this fragmented debris will spread out over time to orbits at all inclinations [Ref. 5]. This would imperil all LEO satellites, and the snowball effect would continue.

Limiting our focus to LEO will take advantage of operations based from the space shuttle or the space station. The Soviets have only a limited number of rocket launch vehicle configurations, but these systems are launched with greater

frequency than their American counterparts. The effectiveness of removing debris can be increased by focusing on a target type that is present in large numbers and possess uniformity in shape and size. Due to the high usage of discrete angles of inclination, there exists the possibility of "sweeping" these orbits. This provides the ODC with the opportunity to eliminate debris in these trajectories with minimum Δv expenditure. This maximizes the effectiveness of the ODC while minimizing the cost.

3.2 TARGET TYPE SELECTION

Launches from the years 1985 and 1986 were used as the initial guide for possible target types. This resulted in a field of 139 different objects that met the acceptance criteria. These items fell into six broad categories.

1) ROCKET BODIES. Thirty of these second stage rocket bodies from the C-1B rockets are still in orbit. These are all roughly 2200 kg and are 7.5 m long by 2.4 m in diameter. The R.A.E. lists the stay in orbit for these rocket bodies as approximately 600 years.

2) COSMOS OCEANOGRAPHIC SATELLITES. These are roughly 750 kg satellites that are cylindrical in shape and have extended solar panels. The main body is 2 m in length by 1 m in diameter. There are four currently in orbit.

3) COSMOS NAVIGATION SATELLITES. These are roughly 700 kg in mass and are 1.3 m long by 1.9 m in diameter. There are ten currently in orbit approximately 1000 km up and are not expected to reenter earth's atmosphere for 1200 years.

4) COSMOS FERRET SATELLITES. Roughly 40 kg in mass each. Several are deployed from a single launch vehicle. They are spherical and are approximately 1 m in diameter. In four separate launches, 30 of these satellites have been deployed.

5) SPECIALIZED COSMOS AND MISCELLANEOUS SATELLITES. These are 16 satellites that do not fit into the previous categories or were missing more precise information.

6) FRAGMENTS. Several satellites have large amounts of debris associated with them and make up the additional items. It would seem that two satellites, Cosmos 1656 and Cosmos 1806, have had significant breakup since 1986.

Both the Cosmos ferret satellites and the rocket bodies were present in large enough quantities to be considered worthwhile targets. Rocket bodies were shown to be a more advantageous target for several reasons. The large cross-sectional area made rocket bodies a much more likely candidate to be hit by debris and split up into smaller fragments. The break-up of a rocket body would provide more and possibly larger fragments than the satellites. Removal of a single rocket body would eliminate the potential source for a large number of potential fragments.

While the rocket bodies were substantially larger and more massive than the satellites, rocket bodies had uniform symmetry and were without solar panels and antennas that could affect capture procedures. The final advantage was the fact that almost all rocket bodies currently in use are long cylinders. Once the design concept for the ODC is proven by the capture of a Cosmos rocket body, modifications can be made to the basic design to allow other types of rocket bodies to be targeted.

The selection process was expanded to cover all Cosmos launches[2] up to the year 1988. This expanded search showed there are currently 363 Cosmos rocket bodies in orbit which constitutes about 10% of the Cosmos program's orbiting objects. A further breakdown of the rocket bodies showed that 239 are still completely intact. The second stages of the C-1B rocket accounted for 197 of the 239 rocket bodies. A summary of the Cosmos program's debris can be seen in Appendix A.

As mentioned previously, a goal advocated by this group is the "sweeping" of a single angle of inclination at a time. A heavily congested angle of inclination was seen at 82.9 degrees which held fifty-eight intact rocket bodies which are listed in Appendix B. It is at this location that the Soviets place their navigational

---

[2] It should be noted that the Cosmos program performs both civilian and military functions.

satellites. There are always ten active satellites, six civilian and four military, in orbit. The navigational satellite's life expectancy of only thirty months has contributed to this region having a large number of "dead" satellites and rocket bodies. Figure 3.1 shows how, other than the two satellites which overshot their planned orbits, these satellite are clustered closely together.

By the year 2000 this navigation system will be phased out reducing the use of the C-1B rocket [Ref. 20]. Even if the system is phased out on time, approximately forty more replacement satellites and their associated second stages will be placed in this already crowded region. The rocket bodies between 990 km and 1010 km at 82.9 degree angles of inclination will offer an excellent target area for the first ODC missions as shown in Figure 3.1[3].

---

[3] The information compiled for this section cannot be individually referenced to separate sources. In general, most of the early selection information was provided by the R.A.E. Tables. The R.A.E. Tables presented the size, rough configuration, and orbital location information on the debris. This information was compared to functional information and outline pictures presented in the 1987 edition of The Soviet Year in Space to make final classification decisions. The Satellite Situation Report provided the number of fragments and the most current orbital location data used through this report.

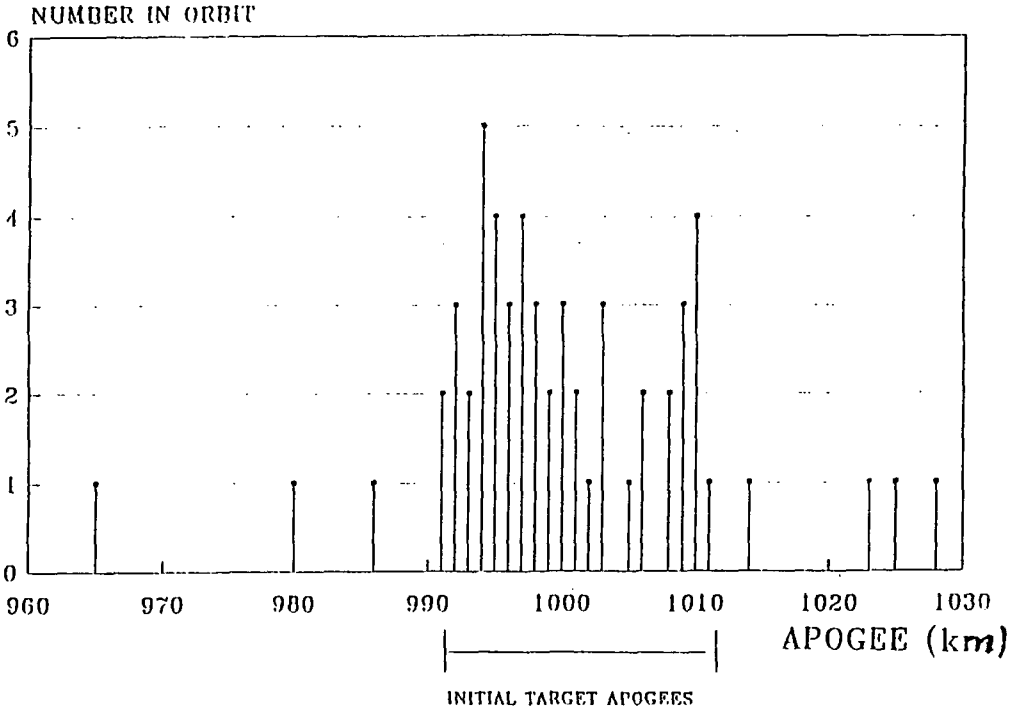

Figure 3.1 - Frequency of C-1B Rocket Bodies

4. ROTATIONAL MOTION ANALYSIS OF TARGET

The motion of a tumbling object in orbit can be broken into two parts; rotational and translational. According to the functional requirements, the rotational energy must first be eliminated, and then a change in momentum is induced to the debris, providing a translational motion. The following analysis was used to develop our design criteria.

The primary objective of this analysis is to describe the rotation of rocket bodies and to determine the energy and torque required to eliminate the rotational motion. Analysis of rotational motion began last semester. Initially, the group determined that the objective of the ODC would be to capture a piece of debris rotating about two or more axes simultaneously. The Grumman reports on the TSR were designed for a body rotating about is axis of greatest moment of inertia [Ref. 14], i.e., spinning. The implication of axial rotation was based on the longitudinal axis approach the TSR made on its target. With this approach the spin table would only be effective for rotation about the longitudinal axis. After an extensive search for the true rotation of a target a report by Martin Marietta [Ref. 17] was obtained.

An in depth analysis of satellite and rocket body rotation was performed by

Martin Marietta in 1986. Through mathematical modeling and actual observations of a tumbling satellite, it was determined that objects tend to spin about their major axis of principal moment of inertia. This is in the case of the Cosmos C-1B rocket bodies a diametral axis. With this knowledge the design team of the ODC could begin. The Martin Marietta report described how several satellites lost attitude control and power resulting in an uncontrolled tumbling motion. After a short period of time (within two weeks) the motion had reduced to a single spin about a diametral axis [Ref. 17].

The next question to be answered was in what direction was the axis of rotation pointing. Ideally, for reasons dealing with proximity operations and the problem of plume impingement, this axis would point towards the center of the earth. However, after conferring with Dr. James Cochran of Auburn University, it was determined that a cylindrical body tumbling in orbit will have its diametral axis directed perpendicular to the orbital plane [Ref. 21]. This fact is based on actual examples which Dr. Cochran cited and on mathematical proofs. An analysis of the Cosmos C-1B 2nd stage launcher was made to determine the center of mass, mass moment of inertia, rotational energy, and the torque required to eliminate the rotational energy. Due to an assumed time window[4] of 30 minutes the process of

---

[4] A time window of 30 minutes was assumed by Grumman Aerospace in order to make use of solar lighting and to prevent excessive delay in relaying communications.

eliminating the rotational motion was given a limit of five minutes.

Several assumptions were made when making a mathematical model of the launcher. The rocket body was broken down into three sections; fuel cylinder, thruster mechanism, and nozzle. The fuel cylinder and nozzle were assumed to be hollow cylinders and the thruster mechanism was modeled as a solid cylinder. Within each section a uniform mass distribution was assumed. The thruster section is the only component with potential to have a significantly non-uniform mass distribution due to residual fuel. In recent years, any residual fuel remaining in the rocket body is vented once the rocket body has fulfilled its purpose, hence giving some validity to the assumption of mass uniformity in this section. With the exception of total mass and overall dimensions, no breakdown of mass distribution and actual dimensions of the rocket body have been obtained. Due to this fact, further assumptions had to be made on the division of mass within each section and the dimensions of the component.

The largest angular velocity mentioned in the Martin Marietta report was 7 revolutions per minute (rpm) [Ref. 17]. In the report by the University of Texas an angular velocity of 50 rpm was used to allow for a significant safety factor [Ref. 10]. The performed analysis was based on three angular velocities; 7, 20

and 50 rpm. Altering the mass distribution had little effect on the overall results. Therefore, only one mass distribution will be presented. Figure 4.1 depicts the basic mathematical model. The mathematical analysis was performed on MathCAD version 2.57 (Appendix C). The energy required to stop the rotational energy is small compared to the thrust capabilities of the OMV. .

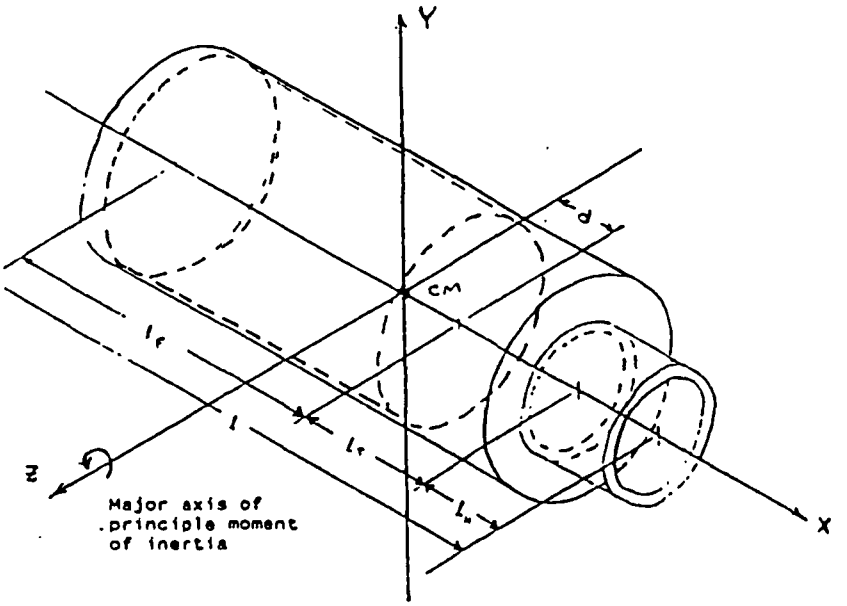

Specifications:

Mass.....2200 kg
Length.....7.5 m
Body Diameter.....2.4 m

Assumptions:

Can be divided into 3 basic sections
- Fuel cylinder
- Thruster mechanism
- Nozzle
Mass is evenly distributed in section

Figure 4.1 - Idealized Model of Cosmos C-1B Launcher

5. EVOLUTION OF DESIGN

The design goal was to develop a conceptual design for an unmanned vehicle to operate in LEO, maneuvering to within range of a debris target, ultimately capturing and controlling the target in order to dispose of it.

With the continuing literature search, it was found that there already existed technology related to the goal of space debris capture. One important tool was the OMV proposed by NASA [Refs. 12,13]. The main objective of the OMV was to extend the range of the Space Shuttle. It was to be carried into LEO by the shuttle and used to retrieve satellites from higher orbits. In addition to this function, other mission scenarios were envisioned to be carried out by the OMV. One such mission was debris retrieval; although there were no details as how this was to be carried out.

It was immediately evident that the OMV would make an excellent vehicle, providing propulsion, communication, and power for whatever design was developed. Therefore, the remaining challenge for the design team became the development of a grappling device, which could be attached to the OMV and facilitate the capture of spinning or tumbling debris.

Further investigation led to the discovery that NASA had subcontracted two

companies to design a "kit" that could be attached to the OMV for the purpose of capturing satellites. One of the companies, Grumman Aerospace, developed the Tumbling Satellite Retrieval (TSR) system to the prototypical stage. The TSR consisted of a spin table in order to match the spinning motion of a satellite, combined with three robotic arms[5] used to close around and capture the satellite. Although their report stated that it could be used to capture debris, most of their work was geared towards the capture of spinning satellites [Ref. 14].

By this time it was decided that the intended debris target would be the Soviet Cosmos C-1B second stage rocket body. For this reason the design of a capturing mechanism would be based on the dimensions and behavior of this target.

At this point, the design team divided into two design groups. One group's goal was to adapt the existing TSR design to the Cosmos C-1B target. Due to their bulk, it was decided that the present design of the TSR was not capable of capturing these targets. The second team would attempt to design a capturing device that was not based on the TSR concept, but that could be used in conjunction with the OMV.

---

[5] Other capture devices designed by Grumman Aerospace included an Apogee Kick Motor capture device, Snare End Effector, and standard Flight Support System capture device. The three arm capture device, however, most closely resembles our design.

A critical problem that existed at this stage of ODC development was the lack of definite information on the rotational behavior in orbit of these rocket bodies. Although information on orbital location was available, the direction of rotation was unspecified. The effect of a spinning motion, rotation about the longitudinal axis, or a tumbling motion, rotation about a diametral axis, would have a significant impact on the final design. A spinning motion was the initial assumption made by the design groups.

In attempting to develop a non-TSR based design, many ideas were investigated. The first design was the use of the Remote Manipulator System (RMS) currently used on the space shuttle. Such an arm could be attached to the OMV. However, the grappling device on the end of the arm would have to be redesigned as the rocket bodies we intend to capture have no probe fixture on them. The current RMS grappling device requires the intended target to have such a fixture. This design is shown in Figure 5.1.

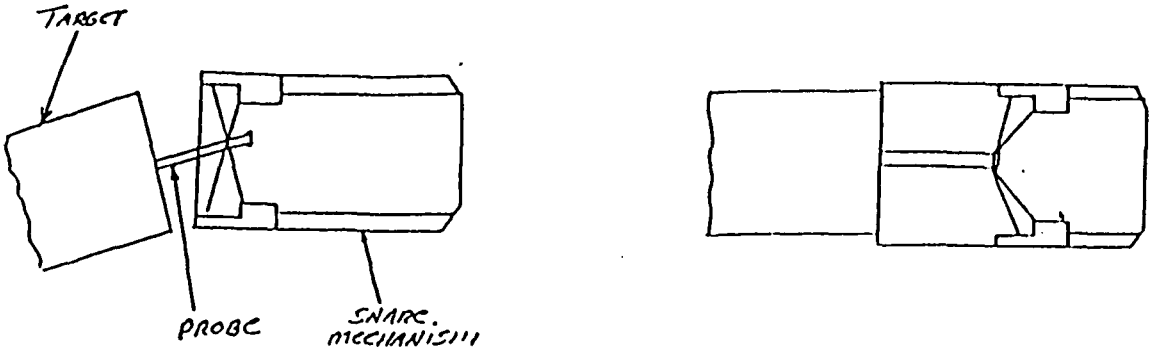

Figure 5.1 - Shuttle RMS End Effector

Another concept investigated was the use a of net mechanism. Either a rocket propelled net that could be launched from the OMV or a butterfly type net that would be attached to the OMV, and are shown in Figures 5.2a and 5.2b. The greatest advantage of these soft capture designs was their relative simplicity. However, there was thought to exist a greater disadvantage in that there was less control with this type of device. That is, the point of contact with the target was less predictable. Making uneven contact with a spinning or tumbling rocket body

could cause the motion of the body, which had a stable uniaxial spin, to become erratic. This in turn might result in the tangling of the net device, which could have the catastrophic result of the payload wrapping itself up in the net and colliding with the OMV. For this reason the concept of using nets was abandoned.

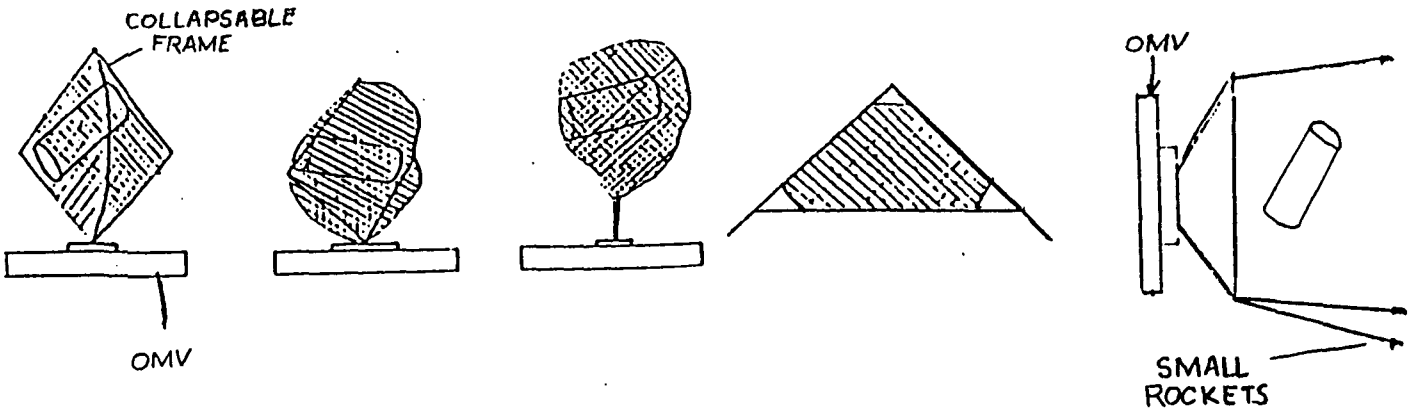

a) b)

Figures 5.2 a) & b) - Net Mechanism Proposals for ODC

At this point, another idea considered was that of the design of a device containing a continuous wide loop of flexible material that could be maneuvered around the target and slowly reeled in. Friction between the loop and the rocket body would slow the spinning motion of the target to facilitate its capture. This is seen in Figure 5.3.

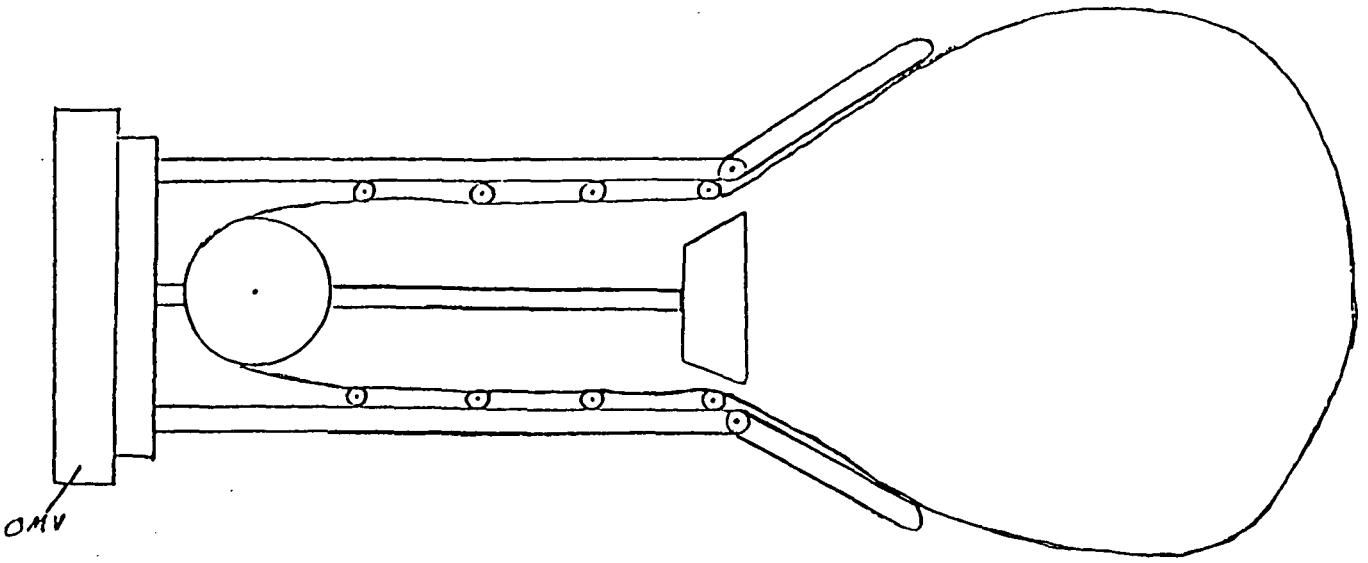

Figure 5.3 - Loop Proposal for ODC

However, at about this time it was determined that the assumed spinning motion of the targets was incorrect. In discussions with Dr. James Turner of NASA, who was the supervisor of the TSR project at Marshall Space Flight Center [Ref. 22], it was found that the rocket bodies would have a tumbling motion. Because the RMS and continuous loop mechanisms could not handle this tumbling motion they could not be used. Therefore, due to time constraints on the project, it was decided that the best course of action would be to have a single design group whose objective would be to adapt the TSR device to capture a

tumbling rocket body. In order for the TSR to be effective to this end, significant redesign was required. The spin table would still be used to match the tumbling motion of the target, but the arms, actuators, and end effectors would have to be redesigned. In addition, some sort of braking mechanism would have to be developed to stop the tumbling motion of the target once it was captured.

The redesigned device is to be known as the Orbital Debris Collector (ODC). The OMV and ODC assembly is to be known as the Rocket Body Retrieval Vehicle (RBRV). The space shuttle and RBRV are the basic components of the capturing system. The shuttle will deliver the RBRV into low earth orbit. The OMV will provide all propulsion and maneuvering for the ODC; including reaction and attitude control as well as the despin stabilizing torque. In addition, the OMV will provide all data management, power, guidance, and navigation as well as serve as the link with ground control [Ref. 14]. The ODC will provide the means to capture the target and bring it under control. This constitutes the evolution of the ODC design.

6. CONCEPTUAL DESIGN

6.1. SPIN TABLE AND ASSOCIATED EQUIPMENT

The conceptual design developed by the Old Dominion University ODC team is shown in Figure 6.1. This design graphic was developed on CADAM 3-D as a concept study. Some preliminary work will be presented in the following sections covering what has been done by the ODC team concerning the spin table, shaft sizing, brake mechanism, ODC arms, camera and lighting, thermal protection, and maintenance.

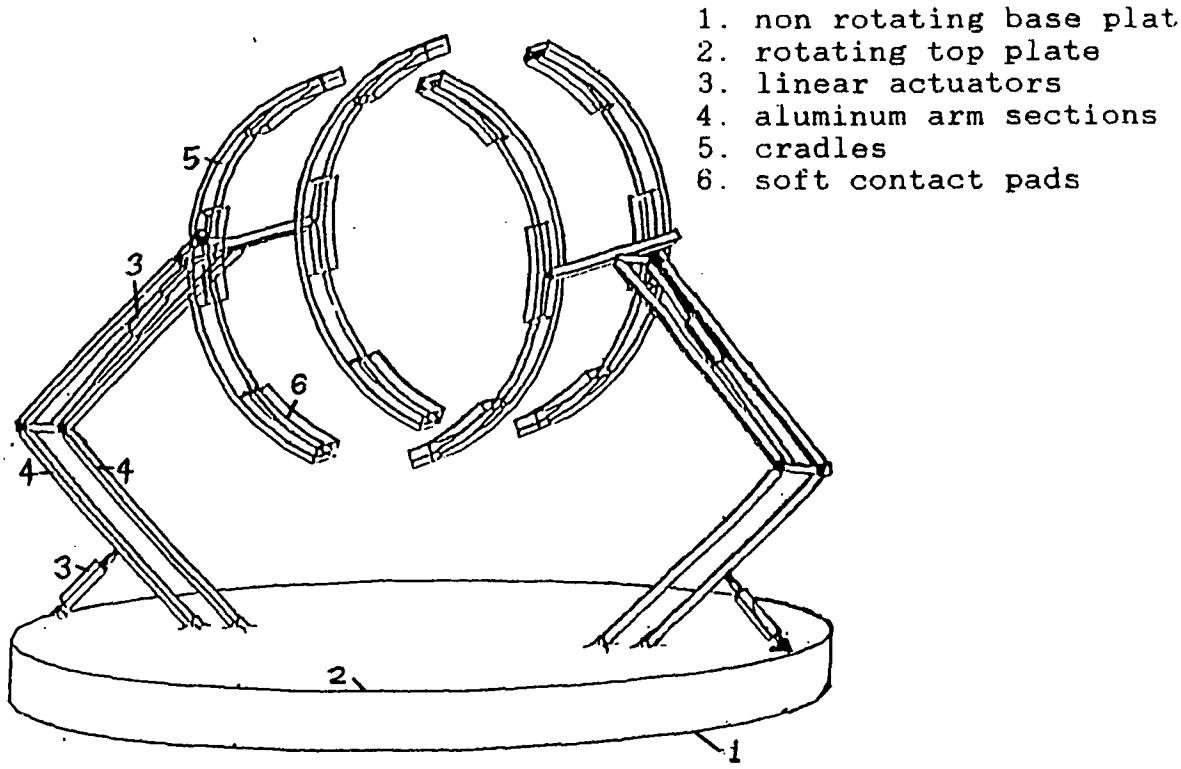

Figure 6.1 - ODC Conceptual Design

6.1. Brakes

One portion of the ODC project that was able to make use of existing work is the spin table and associated equipment developed and tested by Grumman Aerospace as part of their TSR. The spin table is a flat plate approximately 4.5 m in diameter that rotates to match the spin of an object in space. This spin table will provide the base for the ODC's arms. An electrical motor will provide the torque needed to bring the spin table to a rotational speed equal to the rotating rocket body. Torque will be transmitted by a shaft coupled to the motor shaft and welded at the spin table. Finally, a brake mechanism will bring the rotating spin table and the captured rocket body to a halt.

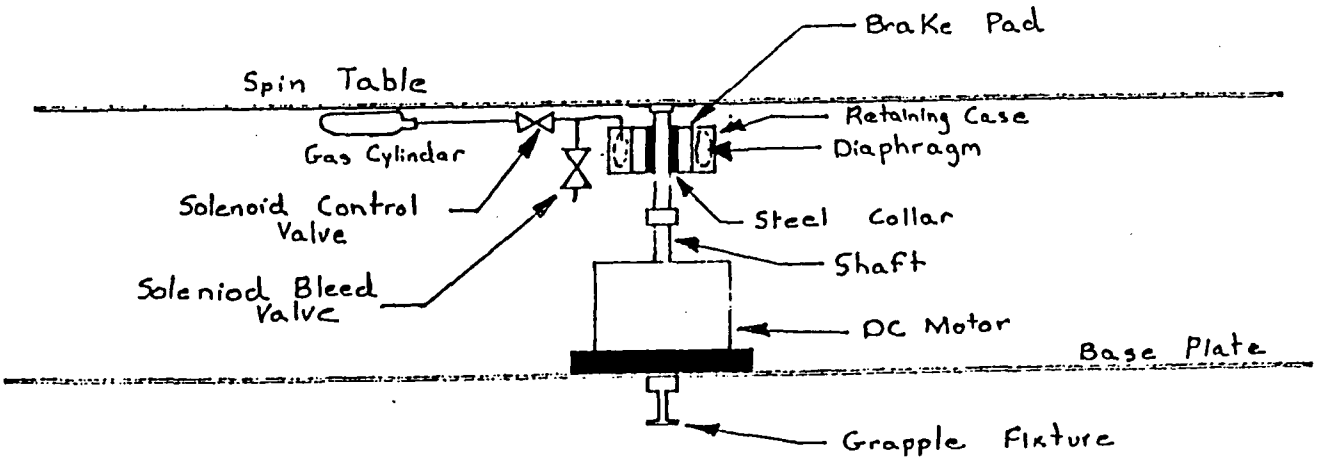

Figure 6.2 - Braking Mechanism for Spin Table

The main requirement of the braking system on-board the ODC is to bring the rotating spin table, the arms and the rocket body to a complete stop within the previously mentioned time frame. This five minutes of the thirty minute capture window has been allotted to bring the satellite under control prior to start-up. Braking operations in space provide interesting challenges. The main problems are providing and countering a braking force in a zero gravity environment. Thermal cycling would effect hydraulic systems which are normally used to provide the braking force. Networks of springs could be used to secure and release the brakes, but the system would be difficult to design and hard to service in space. Magnetic current and eddy current brakes were considered, but these are currently "designed in the laboratory using theory and trial and error" to overcome inadequate knowledge of field effect between conductors in a close area [Ref. 23]. Also, there is a limit of only five kilowatt hours of available electric power to support all functions aboard the RBRV.

To avoid these problems a brake using compressed gas to provide friction to a collar was chosen as a braking system. The system is depicted in Figure 6.1. To activate the brake, the solenoid control valve would open and release compressed gas to expand the diaphragm. The diaphragm can only expand by forcing the brake pads toward the shaft. As the brake makes contact with the

shaft, the brake will impose a resisting torque to the shaft. When the shaft comes to a stop, the pressure can be held to lock the shaft and prevent rotation during orbital transfer. Once the RBRV is ready for another capture the solenoid control valve will close and the solenoid bleed valve will open to release the pressure on the diaphragm and release the brake. The system has the advantage of fewer mechanical parts that could fail during a mission. Leaks could potentially be a problem, but if the leak could be traced by a gas monitor and patched in space. A patching procedure would be easier to accomplish by a suited astronaut than replacing broken springs. If the system did not leak during final checkouts on earth, the spin table would shield the system from projectiles that could puncture it while in space, limiting the opportunity for puncture by debris.

The governing equation for brakes and clutches is

$$t_1 = \frac{I_1 I_2(\omega_1 - \omega_2)}{T(I_1 + I_2)}$$

where t_1 = the stopping time in seconds,
I_1 & I_2 = the moments of inertia for the moving and non-moving part respectively,
T = torque required to stop
w_1 - w_2 = the velocity difference [Ref. 24]

Since the rocket body rotational velocity may be from 0 to 50 revolutions

per minute (rpm) and the moments of inertia should be known, the torque in N·m may be found.

Also, the energy of the system can be determined by

$$E = \frac{I_1 I_2 (\omega_1 - \omega_2)^2}{2(I_1 + I_2)}$$

where E = energy (J) produced by the braking action [Ref. 24].

Notice this equation is dependent only on the moments of inertia and the velocity difference and could be used for any braking method. But more importantly, it is independent of torque and therefore time. This provides us with the amount of heat that will have to be rejected over the course of the braking action.

By using the design values for the rocket body moment of inertia, and the arms used to capture the rocket body, I_1 can be determined. Modeling the OMV as a solid cylinder, 4.5 m in diameter and 2 m in height, of constant density and assuming that the non-moving moment of the ODC is roughly 75% of the moving portion, I_2 can also be estimated. By taking different rocket body rotational rates, the torque needed to stop rotation and the energy produced can be calculated. A sample calculation has been provided in Appendix D. Figure 6.3 provides a summary of the values found. This heat load would have to be added to the other internal heat loads and the external load from solar radiation to determine the heat transfer during the capture procedure. Additional studies should be made into this

problem and the related question of how to reject the heat produced during braking.

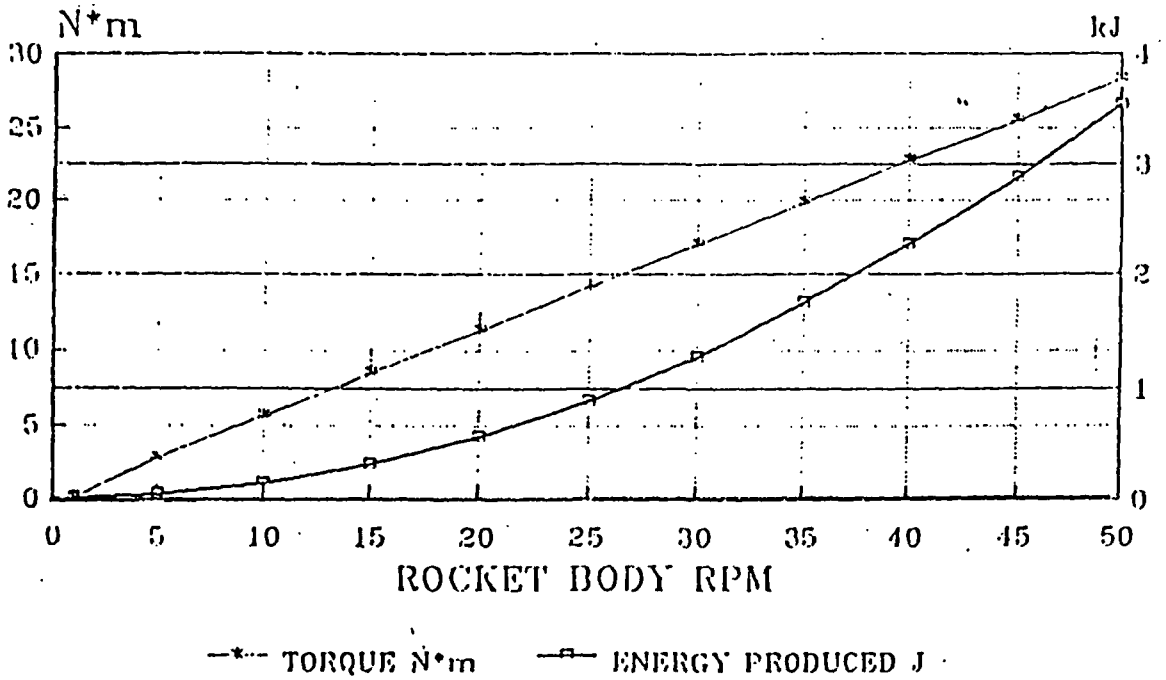

Figure 6.3 - Torque Required to Stop Rotation & Energy Produced as a Function of Revolutions per Minute of Rocket Body Rotation

With the known torque values, a more detailed study of the brakes can be made. The first step will be to determine the width of the brake. This may be found by

$$w = \frac{(T/n)}{2\mu p_{MAX} r^2 \sin\left(\frac{\phi}{2}\right)}$$

where n = number of brake pads,
p_{max} = maximum design pressure of the brake material,
μ = coefficient of friction for braking material
ϕ = brake pad arc
w = brake shoe width
r = shaft diameter [Ref. 23].

With the band width determined, the braking force and therefore the compressed gas pressure may be determined. The braking force is therefore:

$$F_s = p_{max} r w(\phi + \sin\phi)$$

where F_s = Braking Force.

This force will then be applied over the surface area of the diaphragm. If it is assumed that a distance is needed to support and bond the brake pad to the diaphragm, the diaphragm pressure becomes

$$p_{dia} = \frac{F_s}{\pi r_{eff}^2}$$

where p_{dia} = pressure in the diaphragm
r_{eff} = the inner radius of the diaphragm [Ref. 23].

A sample calculation has been computed in Appendix D which will show that for the highest assumed rotation of 50 rpm, the brake will need to have a width of .251 m (9.88") and will require a gas pressure of 534.5 Kpa (77.57 psi). It can be seen that the width of the shoe, braking force, diaphragm pressure, and the torque are all linearly related and relatively small. It should therefore not be difficult to design a braking mechanism as described to overcome these forces.

These braking requirements fell within acceptable levels for the opposing OMV thrusters.

6.3. ODC ARMS

An arm of the ODC consists of two four-bar linkages of approximately equal length. At the end of the second linkage is the cradle which will make contact with the rocket body. The purpose of the dual linkages is to keep the motion of the cradle parallel to the spin table and to allow for rectilinear motion. The cradles were designed to contact the rocket body at four or more points. This should reduce the potential for tank rupture. Pads will be placed on the cradle arm to allow for soft and even contact. The cradle was designed to provide a large moment arm, allowing a substantial torque to be conveyed to the rocket body without causing the rocket body to flex or bend.

An analysis of potential materials resulted in the selection of Aluminum. Kevlar and Spectra Fiber were investigated but were rejected due to the anisotropic nature of both materials and the difficulty of modeling. Spectra Fiber is also

relatively new and information on this material is limited. Aluminum offered high strength, light weight, low cost, availability, resistance to corrosion, resistance to the effects of atomic Oxygen, desirable thermal properties and ease of manufacture. A tubular design of the arm section was determined to be the best option because of the optimization of weight to torsional load resistance. A NASTRAN finite element analysis was performed on several inner and outer diameter configurations. A configuration with an outer diameter and inner diameter of 8 and 6 cm respectively of all arm sections, was determined to be well suited for the ODC. These dimensions and configurations have been analyzed using NASTRAN/PATRAN and the with the output file of the PATRAN deformed plot are shown in Appendix E. With these dimensions the factors of safety were extremely high, with none less than 1000. Smaller diameters were not analyzed due to the fact that there is a potential that the highest stresses will occur during the launching of the ODC.

6.4 MECHANISMS OF ODC ARMS

The main requirement of the ODC arms was that it had the ability to perform rectilinear motion upon its final capture phase. It is inherent that a

straight line motion along the centerline of the rocket body, as shown in Figure 6.4, would have the most accurate motion, as no anticipation of landing point has to be made by the controlling mechanisms and/or pilot. This ease of pilot operation is essential as it is baselined for the RBRV to be "man in the loop" operated in the final phase of operation.

The ability to perform rectilinear motion also has the advantage that the vertical distance, i.e. the distance labelled H in Figure 6.4, can be adjusted quite easily. This is of great advantage to the ODC which may have to maneuver around exterior ribs, a standard feature, on the Cosmos launcher.

The final major reason for requiring rectilinear motion is as previously mentioned, final approach must be as accurately controlled as possible, in order to place the cradle in the appropriate position on the Cosmos C-1B launcher. The appropriate position on the launcher is dictated by the center of rotation. Placing the cradle at a point far enough away from the optimal contact points may impinge on the uniform one dimensional rotational motion, ultimately resulting in a catastrophic multi-dimensional rotation causing the destruction of the RBRV. To achieve this rectilinear motion, a double four-bar mechanism was designed, with appropriate linear actuators as shown in Figure 6.1. The logic behind the selection of the four-bar mechanisms lies in the necessity to keep the orientation of the

cradle pointing colinearly with the rocket body centerline. As shown in Figure 6.4 the cradle is always oriented in the same manner, as a result of using the four-bars. A complete analysis of the position and velocity of the cradles as functions of the actuators is given in Appendix F. The placement of the actuators was determined by mass considerations and by ease of operation. No model types are suggested, but it is envisioned that these actuators electric motor driven linear actuators. Their required extension range and velocity requirements are also provided in this appendix.

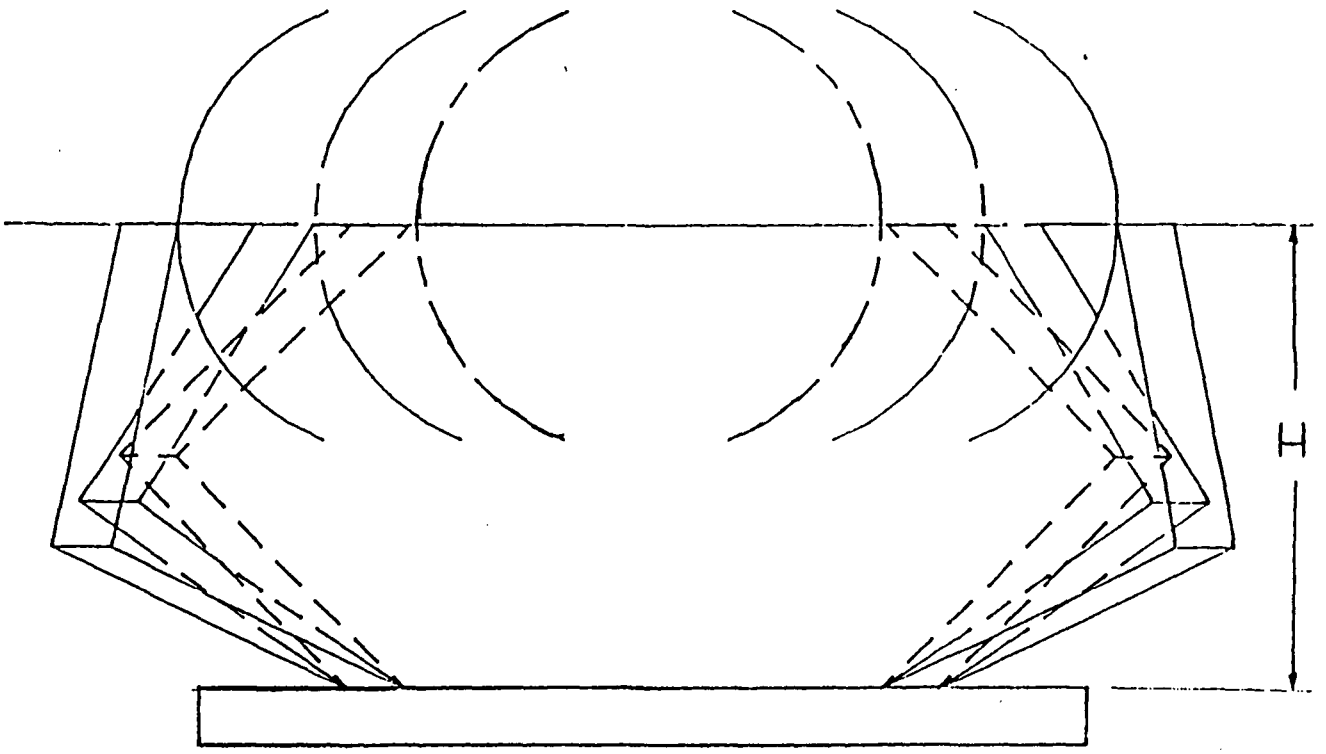

Figure 6.4 - Rectilinear Motion of ODC Arms

6.5. CAMERA LOCATION

TV cameras will employed during all phases of the interception operation. The OMV's tracking and camera systems will not be discussed here, but it is envisioned that the OMV will provide the ODC with this information up to thirty meters away from the target. However, after the ODC will be required to possess its own camera system.

This system involves both ODC arms having a camera mounted on a boom structure located near the base of the cradles. The booms are sized and oriented in such a fashion as to see around the cradles. The cameras will offer a close range view of the capture, just prior, and at the point of contact. In addition, these cameras will have the ability to rotate in order to obtain a wider angle view of the contact area. Located at the center of the spin table, somewhat like the TSR idea [Ref. 14], is another camera which will give added input to the controller concerning the axial aligning of the spin table and C-1B. This camera has the ability to rotate independently, matching the rotational speed of the rocket body prior to the activation of the spin table, so that the ultimate spin table alignment could be achieved with the minimal energy consumed. With these three cameras being used, a successful is possible. However, the addition of one more camera located at the outer edge of the spin table, 90 degrees from where the arm

mechanisms attach to the spin table would be helpful. This added camera would give the pilot another viewing angle to ensure no relative rotational motion between the rocket body and the spin table. A point of note, is the existence on the present OMV design of two non-spinning, off-axis cameras which would facilitate viewing the entire capture area of interest [Refs. 12,13].

6.6. THERMAL PROTECTION

In performing an adequate thermal analysis of the RBRV, it was evident that many important parallels exist between the RBRV mechanism and the current Shuttle RMS. Both of these operate in the same LEO environment, both have similar components, perform similar movements, and have similar applications. Precluding a formal analysis, it was determined that thermal protection similar to the RMS should be incorporated into the ODC. The materials and components of the RMS have already undergone extensive hours of research, design, and analysis, and their effectiveness has been proved on numerous occasions by actual mission testing. The OMV has its own thermal protection, and any interface between the OMV and the ODC will be designed to minimize heat transfer.

The RMS thermal control systems are comprised of both active and passive

systems. The active system consists of 26 heaters on the arm, with a total power consumption of 520 Watts. These are placed at various strategic locations, primarily around joints and motors. They are controlled by 12 thermistors along the arm and are activated when the temperature goes outside of the interval between 14 °F and 43 °F. The passive system consists of thermal coatings and layered insulation blankets. A special white paint is applied to all exposed areas and the blankets are wrapped around the arm, making sure to not restrict the movement of the arm, and are attached with velcro tape [Ref. 25]. The multi-layered insulation blankets consist of five layers of goldized kapton film, with alternating layers of spacer material. This protects the arm from deep space cold and minimizes the reflected solar energy from the arm.

Because of the many similarities between the ODC arms and the RMS, and the effectiveness of the RMS thermal protection, it has been determined that these precautions should prove sufficient to ensure the ODC surfaces will be protected from the extreme thermal environment of space.

6.7. CONCEPTS FOR IMPROVED LIFECYCLE PERFORMANCE

An early emphasis was placed on the capability to perform a large number of debris collecting missions during the ODC lifetime. The lifecycle of the ODC will be affected by several factors including

1) Wear on portions of the mechanisms (pads, arms, collars, brakes, and actuators).

2) Damage to sensory equipment (cameras, lighting, and laser rangefinder) by small debris fragments.

3) Severe damage to the ODC during the capture procedure (misalignments of arms or spin table shaft, actuator or brake failure, or spin table motor burn out).

Analyzing the possible ways the ODC might fail has lead to some recommendations on serviceability. An important point to remember is that the all of potential repairs on the ODC should be capable of being performed during EVA. This will require modular design and quick disconnect fittings to be used throughout the design wherever possible. Components subject to wear should be capable of modular replacement by suited astronauts. Since some debris in space is the actual fasteners and tools released by previous missions (mission debris), care must be taken so that fasteners and other components remain an integral part of the ODC or failed module. Pads, for example, will need quick disconnect type

fittings for the pressurization system and a clip to hold the pad in place. The brakes could be removed by separating the internal and external portions of the brake. After sliding the internal portion off the collar, access could be gained to replace the brake shoes or patch the inflatable collar.

Sensory devices, due to their external location and delicate nature, should be easily replaceable. Unfortunately, their location will expose them to small space debris and their function prevents the sensors from being shielded effectively. While direct damage is a threat, jarring and vibration from the capture procedure should not be allowed to effect the mission. It will be necessary to design the arms to break away from the spin table if the table cannot control the braking, or an unexpected force is encountered. Modularized arms could be used to quickly replace a lost arm .

7. DISPOSAL ANALYSIS

7.1 TRANSLATIONAL MOTION ANALYSIS

Once the rotational energy has been dissipated from the debris, the next step is disposal of the object. Since the targeted debris is at quite a high altitude ($\approx$1000 km), and has a long orbital life (up to 600 years), the goal will be to impart a change in velocity (Δv) on the body to induce an orbit transfer downward thus greatly reducing its orbital lifetime in space due to an increase in atmospheric drag. A graph of altitude vs. orbital life without propulsion is included in Figure 7.1 [Ref. 26]. The result is a straight line showing a direct linear relationship between the altitude and orbital life. Due to the already high level of development and high accessibility of atmospheric entry concepts, a detailed mathematical model is not included in this report. However, the general method of deorbit as well as several useful relationships such as skipback phenomenon are discussed. Finally, a recommendation for a most efficient course of action is defended.

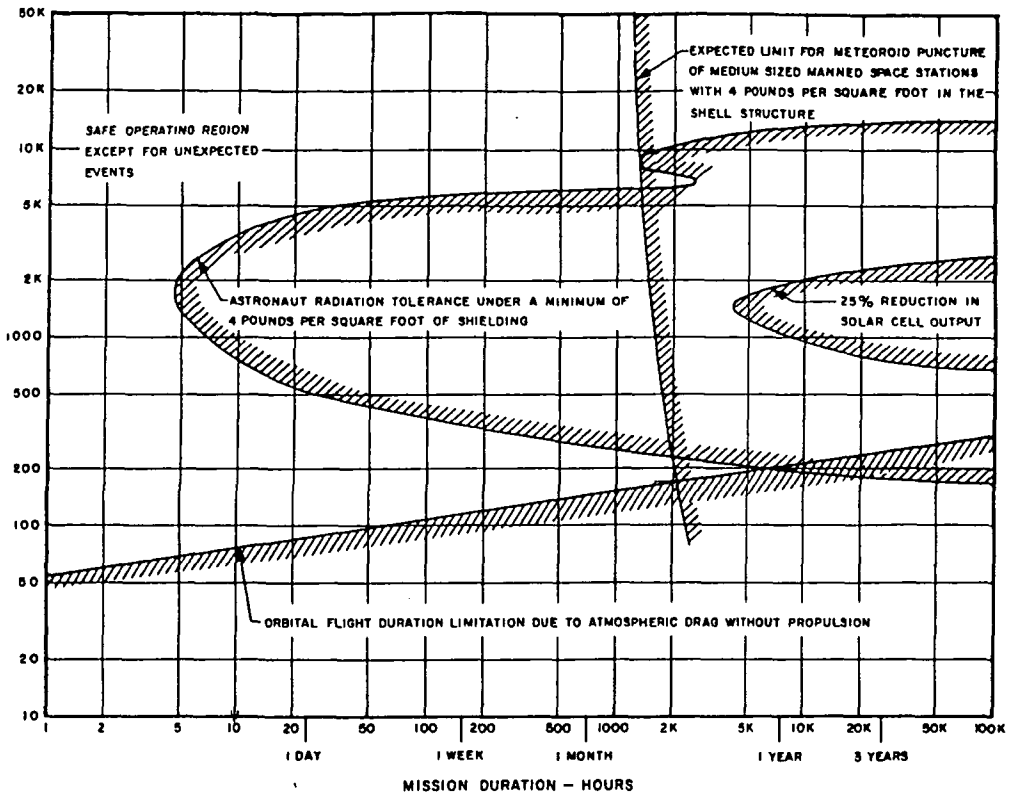

Figure 7.1 - Altitude vs. Orbital Life

7.2 ΔV ANALYSIS

A Δv will be imparted to the debris to induce a decay in orbit. Two main assumptions must be understood for the following discussion. The first assumption is that the rocket body is traveling in a circular orbit. This assumption can be made due to this orbits near zero eccentricity (e =0.003) [Ref. 19]. The second assumption is that only co-planar orbit transfers will be completed.

The actual deorbit process is quite simple to understand. The thrusters of

the OMV will deliver a Δv to the rocket causing it to fall into successively decaying parabolic orbits. From here, due to an increase in atmospheric drag it will continue to fall through the atmosphere either burning up or harmlessly going into the ocean. This process is shown pictorially in Figure 7.2 [Ref. 10].

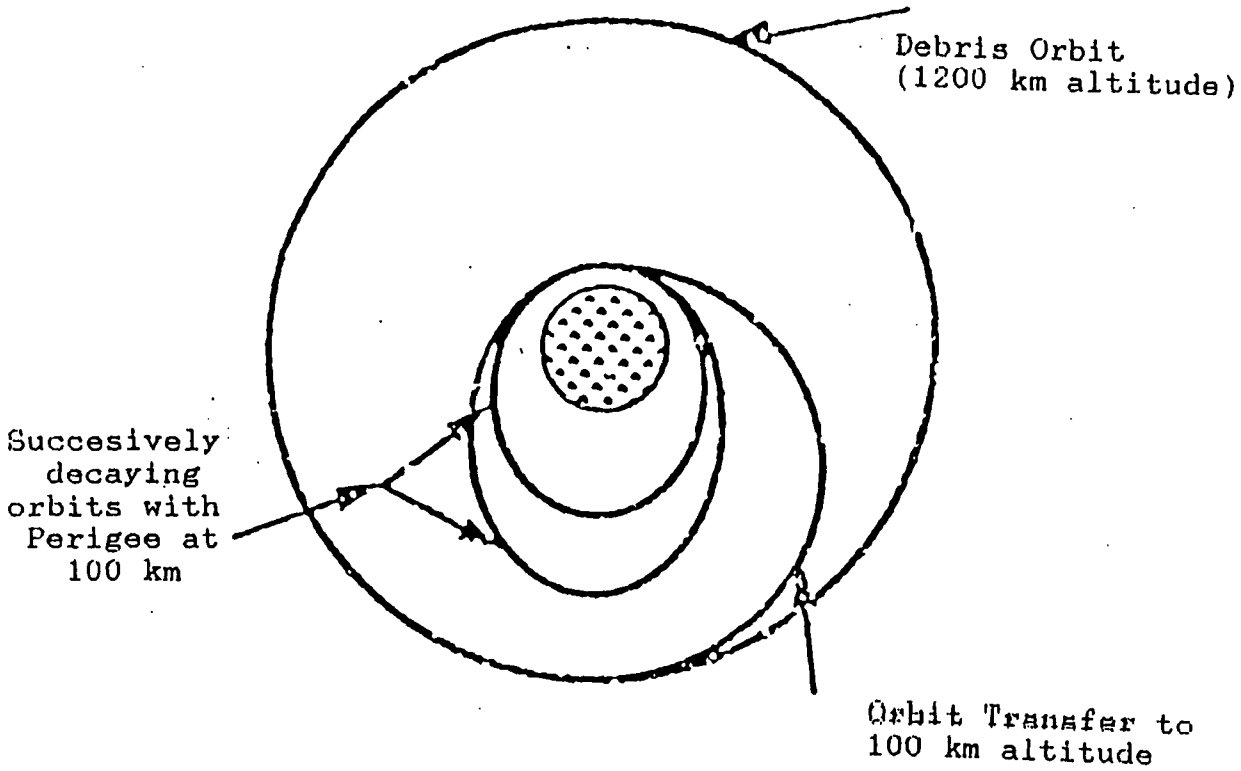

Figure 7.2 - Successively Parabolic Decay

For the following analysis, these variables must be defined:

r = original orbit radius of Cosmos rocket
s = semi-major axis of orbit

p = final perigee after transfer
v_o = debris velocity at original altitude
u = $3.98 \cdot 10^5$ km^3/s^2 (gravitational constant)
v_p = perigee velocity for transfer

The original altitude velocity is given by,

$$v_o = \left(\frac{u}{r}\right)^{\frac{1}{2}}$$

Also, the perigee transfer velocity is:

$$v_p = \{u \cdot [\left(\frac{2}{r}\right) - \left(\frac{1}{s}\right)]\}^{\frac{1}{2}}$$

From here, the difference of the two gives the necessary Δv, or,

$$\Delta v = v_o - v_p$$

To use an extreme case for an example, an original altitude of 1200 km can be reduced to 100 km thus reducing orbital life from nearly 600 years to about 7 hours. After completing the above calculations, a necessary Δv to achieve this transfer is found to be 434 m/s. Or in other words, the velocity of the debris must be reduced from 6950 m/s to 6516 m/s.

Continuing, an ideal Δv equation can be used [Ref. 10];

$$\Delta v = v_e \cdot \ln\left(\frac{m_o + m_r}{m_o + m_r - m_f}\right)$$

where:

v_e = exhaust velocity of the OMV
m_o = mass of RBRV (about 9500 kg)
m_r = mass of debris = 2200 kg
m_f = mass of fuel burned = 2041 kg (1/2 capacity)

Solving this equation for v_e gives,

$$v_e = \frac{\Delta v}{\ln\left(\frac{m_o + m_r}{m_o + m_r - m_f}\right)}$$

So the necessary exhaust velocity for the controlled orbital decay discussed above is about 2200 m/s. This value falls well within the OMV propulsion limits [Ref. 12].

7.3 IMPORTANT ATMOSPHERIC REENTRY RELATIONSHIPS

Though many variables are at work in atmospheric reentry, a few relationships may prove to be helpful if seen graphically. All graphs relate to the sample orbit change discussed already.

Figure 7.3 is a plot of Δv vs. initial orbit radius. This linear relationship is the same as that of Δv vs. initial altitude except for a magnitude factor.

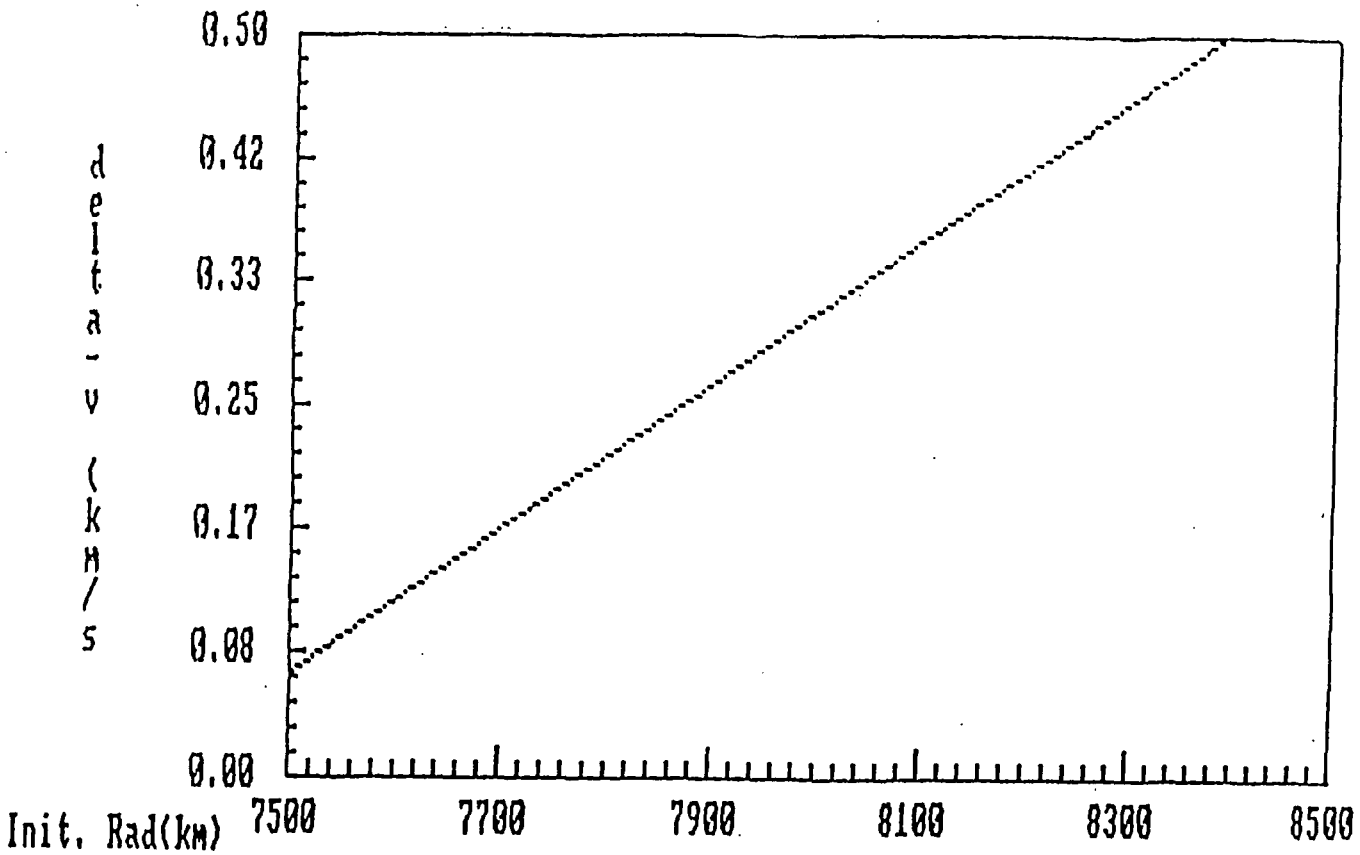

Figure 7.3 - Change in Velocity required to deorbit a body vs.

Initial Orbit Radius

With the Δv values found, the required exhaust velocities can be showed graphically. This relationship also proves to be linear. Exhaust velocity vs. Δv is shown in Figure 7.4.

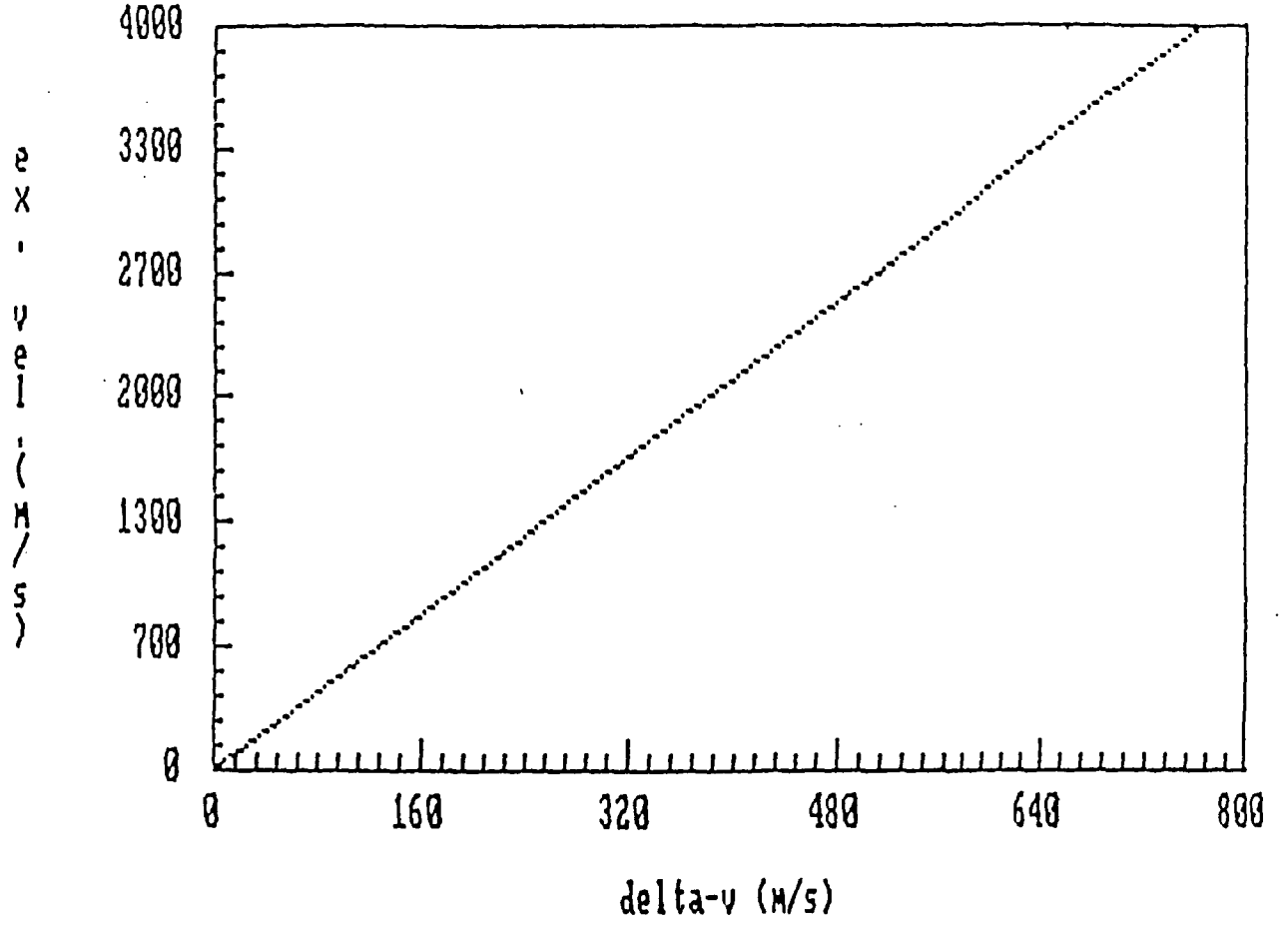

Figure 7.4 - Exhaust Velocity Requirements for Changes in Velocity

Finally, departed kinetic energy is plotted against Δv in Figure 7.4. This parabolic curve demonstrates that from the range of 350 m/s to 450 m/s, energy requirements are from about 133 kJ to nearly 225 kJ.

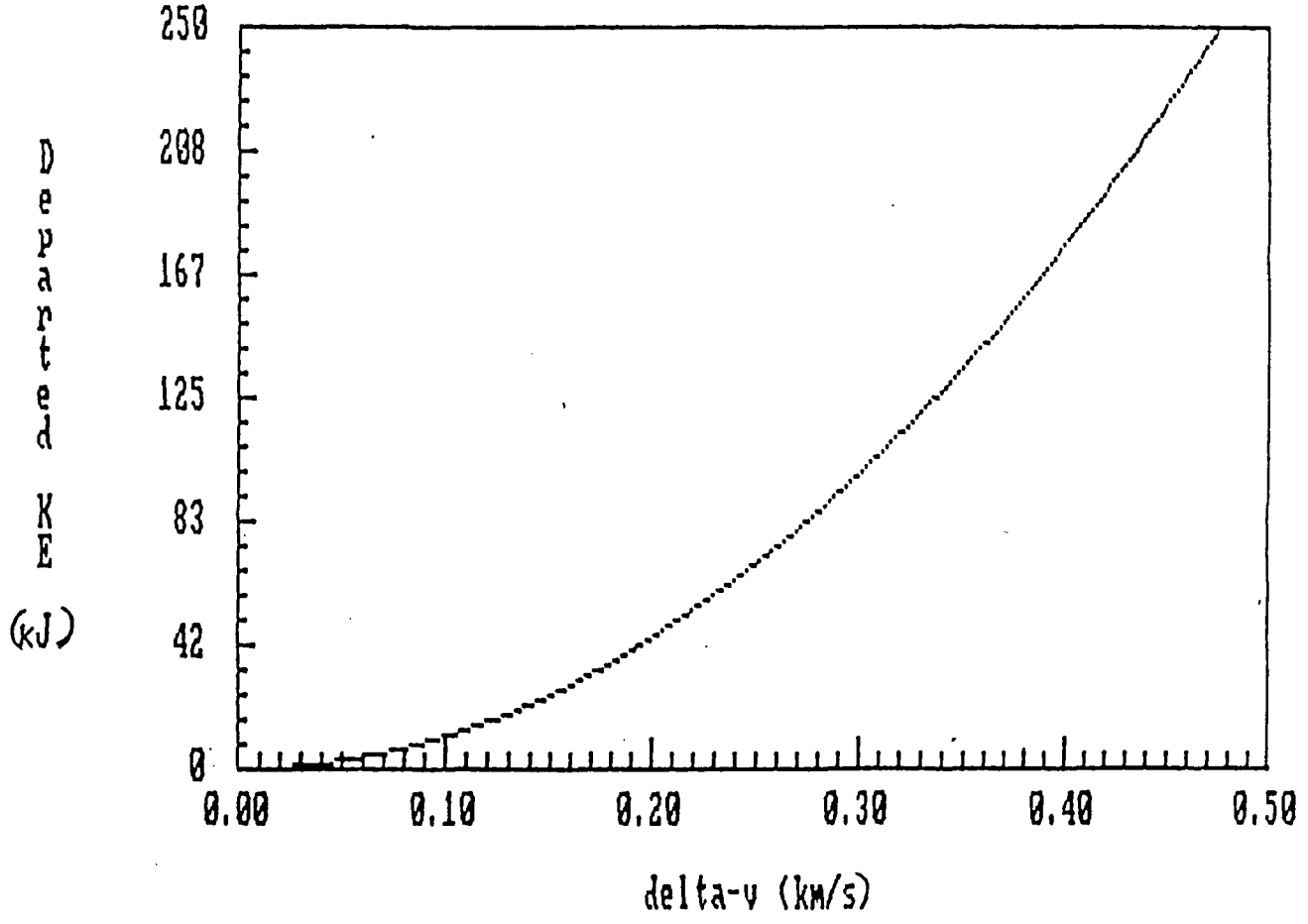

Figure 7.5 - Kinetic Energy Departed vs. Change in Velocity

7.4 SKIPBACK PHENOMENON

Skipback is a naturally occurring phenomenon dealing with atmospheric reentry. A lifting body, while entering the atmosphere with a relatively high velocity and a finite flight angle will tend to bounce back off of the atmosphere at different levels as shown in Figure 7.5. The magnitude of the skip is mainly controlled by the flight angle velocity [Ref. 27] Stated differently, skipback will occur when the lift to drag ratio, l/d, is greater than zero [Ref. 28]. If this ratio is zero, however, the flight angle will continue to increase thus causing the entering body to cut deeper into the atmosphere.

In the case described previously (refer to Figure 7.6), the lift to drag ratio is so small it can be considered zero. Also, the rocket body will enter the atmosphere at a relatively low flight path angle. Therefore, skipback will not need to be a consideration in the above scenario, and the RBRV will not need to escort the Cosmos rocket down to a lower orbit. Once the RBRV transfers the necessary Δv to induce the rocket body into a parabolic decaying orbit, the debris can be released. This is very important since accompanying the rocket body to a lower orbit would require a significant amount fuel to return the RBRV to the original orbit. It has therefore been shown that a significant amount of precious fuel can be conserved by simply disengaging the object after the required Δv is achieved.

This could extend the mission of the RBRV to dispose of a many more rocket bodies.

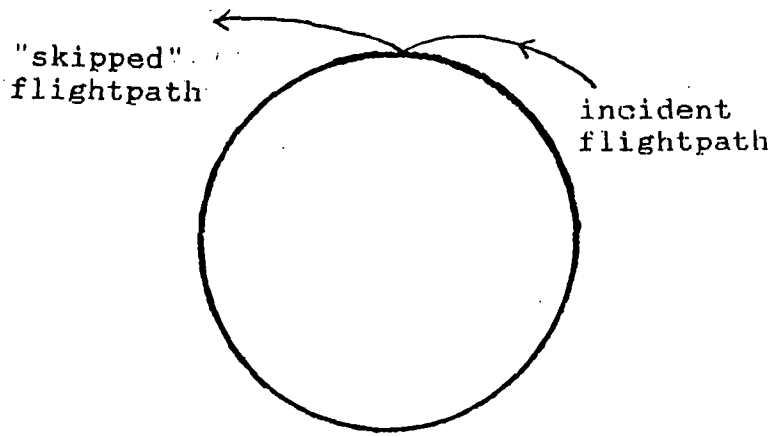

Figure 7.6 - Skipback Phenomenon

8. SAMPLE MISSION

A walk through of critical points during a debris collecting mission was made to validate the ODC conceptual design. This sample mission was also used to refine the design philosophy by eliminating unnecessary service on the collector once deployed. Prior to launch an ODC will be mated to the OMV using the grapple docking mechanism and cantilevered payload attachment points. The ODC will then be connected to the OMV's electrical and telemetry systems. A system check will be made of the RBRV and upon completion of this testing RBRV will be placed in a stowed position on board the space shuttle for launch.

8.1. DEPLOYMENT

The RBRV's launch vehicle will be a NASA space shuttle. The OMV is 14' 8" in diameter and falls within the limits of the shuttle's 15' diameter cargo bay. Since OMV has an overall length of 5' 11" and takeoff weight of 21,000 lbs, the space shuttle's cargo bay capacities would allow the ODC and its support equipment to obtain a maximum of 54' in length and 44,000 lbs [Ref. 29]. The current ODC design does not exceed these limits and can be summarized as follows:

i) TAKEOFF WEIGHT	800 lbs
ii) MAXIMUM DIAMETER (ARMS IN STOWED POSITION)	14 ft
iii) MAXIMUM LENGTH (ARMS IN STOWED POSITION)	15 ft

The space shuttle is currently, and for the foreseeable future, the only vehicle NASA has available to place a 15' diameter payload into space.

The shuttle has the capability to operate in orbits as high as 690 miles which is above the target region of 625 nmi (approx. 1000 km). The shuttle will be used to place the RBRV in orbit below the debris. Deployment point will be at approximately 590 nmi. This height will relieve the RBRV of much of the initial transit fuel expenditures and keep the orbiter out of the main belt of debris. A final computerized system check of the combined RBRV will be made to check for damage from lift off. The OMV currently has a grappling point which will be used by the shuttle's robot arm to deploy the RBRV into space. Once free of the cargo bay the ODC's arms will be deployed. The reason for deploying the arms early in the mission is to determine if any mechanism is jammed while there is still a chance for Extra Vehicular Activity (EVA) repair.

8.2. INITIAL APPROACH

The RBRV will now move towards rendezvous with the target debris using a V-bar approach to debris from the velocity tangential vector as shown in Figure 8.1 [Ref. 30]. This initial approach pattern is necessitated by the orientation of the rotational axis, which was mentioned in the rotational motion analysis section, does not facilitate approach along an R-Bar due to the possibility of plume impingement. The OMV's propulsion system will provide the Δv required and the OMV's guidance system will control the flight.

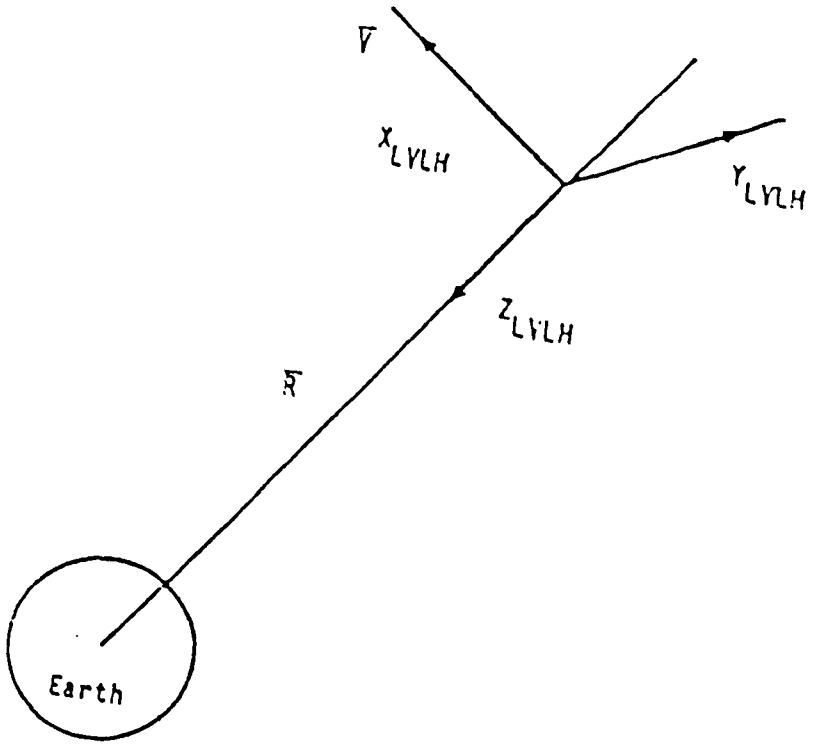

Figure 8.1 - V Bar Approach

8.3. PROXIMITY ANALYSIS

Proximity operations will begin when the radar on board the OMV begins to track the target at a distance of approximately 10 km. Adjustment to flight path at this stage may be made by the OMV or by the operator. When the cameras on board the RBRV begin to register the target at about 1 km, several things will happen. First, the OMV's guidance system will be "slaved" to the person operating the ODC. The operator will control the final approach and the capture procedure. Second, a laser rangefinder will be used to establish the distance between the RBRV and the target. This information will be gathered throughout the capture procedure and presented to aid the operator. Third, the rate of rotation for the target will be determined. A system will have to be developed that can use the camera pictures to determine the rate of rotation of the target. The system

should then calculate the time needed for the spin table to spin-up to a matching speed. Minimizing the time the spin table is in motion will conserve electrical resources for other uses. Fourth, near this point the OMV will switch from using the bi-propellent thrusters to the cold gas system thrusters. With the cold gas system, there is a lessened risk that plume impingement will disturb the target motion.

8.4. CAPTURE

The capture procedure will begin when the operator engages the spin table motor. The spin table will increase speed until matching the rate of rotation of the target. The on board computer will control the spin table's motion at a constant matching spin rate. The operator can verify when the matching spin is obtained by seeing no relative rotational motion in the target through a spin table mounted camera. The RBRV is still approaching the target during the spin up period. The V-bar approach allows the RBRV to approach the target with the least risk of plume impingement. Once the arms are positioned symmetrically on either side of the target and the spin has been matched, the RBRV will cover the last few meters until the target is inside the cradles. The operator will now allow the arms to close. This will bring the cradle pads into contact with the target. When the target is securely in the cradles the despin and deorbit portions of the mission begin.

8.5. DESPIN AND RELEASE

To despin the target the pneumatically operated brake system will begin to slow the shaft speed of the spin table. Once the spin table has stopped rotating, the spin table will be locked in place for transit. The RBRV will then use a

Hohmann transfer back to a lower orbit. The debris will then be released by opening the arms and backing the RBRV away from the debris. The natural drag force on the body will return the debris through the earth's atmosphere for burn-up. As discussed in section 7.4, the skipback phenomenon will not be a problem.

If fuel loads permit, another collection procedure could be attempted. If refueling is required, it could be accomplished at the space station or in conjunction with a fuel transfer system base on board the space shuttle or space station.

9. PHYSICAL MODEL

It must be first mentioned that the model of the ODC is not an exact replica of the actual ODC conceptual design. It is instead, intended to demonstrate the feasibility of the actual design, i.e. to show that the OMV when equipped with the spin table and robotic arms is capable of capturing and controlling a tumbling rocket body.

The model itself is composed primarily of wood. Wood was chosen because of its low cost, light weight and workability. The spin table is represented by a 16" diameter plywood disc to which is mounted a brass shaft. The shaft in turn is mounted to a 36 volt DC motor which by means of a variable power source is capable of spinning of up to 16 RPM. The target, made of a styrofoam cylinder, which is mounted through the center onto a rotating shaft, which is spinning on a similar motor and power source.

The arms of the model are made of wooden spring loaded dowel rods and their operation is controlled by way of a remote controlled motor mounted n the rear of the spin table disc. This motor is used to wind in a thin wire which draws in the arms against the spring tension. This allows the arms to close around the target.

Both the model of the ODC and the target model are mounted on wooden towers. The ODC tower as four wheels and is pushed manually in the demonstration, as the spin table disc spins. The ODC model is then spun at the same rate as the target and a final docking procedure is performed. At this point the arms are closed to close on the target. Once this has been accomplished, the ODC cart is withdrawn whilst holding the target in its cradles. Then, the model's rotation will slow and come to a stop, mimicking the real braking operation of the ODC. Photographs of the ODC model are provided in Appendix G.

10. CONCLUSIONS/FUTURE DIRECTIONS

To conclude, the Old Dominion University USRA design team has successfully proposed a feasible design to capture rocket bodies in LEO. As previously mentioned, a detailed analysis of debris in particularly congested regions justified the targeting of Cosmos C1-B launchers. The ODC arm dimensions were dimensionalized by NASTRAN analyses and a mechanisms analysis was run on MathCad to proved the viability of rectilinear motion. Some sample disposal missions were run and ideas as to the most economical methods of disposal were obtained.

Future directions of this project should include more in depth analyses of debris disposal, in order to develop more detailed fuel requirement data, so that upper mission utility limits could be developed for the RBRV. Attempts should also be made to develop a terrestrial prototype to determine the real operational problem areas, particularly in the control systems of the table and the arms, and the possible effects of misalignments in the final interception phase.

REFERENCES

1. Johnson, Nicholas, L., "Evolution of the Artificial Earth Satellite Environment," from "Orbital Debris From Upper Stage Breakup," ed. Joseph P. Loftus, Jr., Progress in Astronautics and Aeronautics, v. 121, pp. 15-24, 1989.

2. Cour-Palais, B.G., and Crews, J.,L., "Hypervelocity Impact From Upper-Stage Breakup," from "Orbital Debris From Upper Stage Breakup," ed. Joseph P. Loftus, Jr., Progress in Astronautics and Aeronautics, v. 121, pp. 3-13, 1989.

3. Kessler, Donald, J., "Current Orbital Debris Environment," from "Orbital Debris From Upper Stage Breakup," ed. Joseph P. Loftus, Jr., Progress in Astronautics and Aeronautics, v. 121, pp.2-12, 1989.

4. Rex, D., Eichler, P., Soppa, U., Zuschlag, J., and Bade, A., "Space Debris - Origin, Evolution, and Collision, Mechanics," Selected Proceedings of the 39th International Astronautical Federation Congress, Bangalore, India, (October 8 - 15), Acta Astronautica, pp. 209 - 216, 1989.

5. Demeis, Richard, "Cleaning Up Our Space Act," Aerospace America, pp. 10-11, February 1987.

6. Jasani, Bhupendhra, adn Rees, Martin, "The Junkyard in Orbit,"The Bulletin of Atomic Scientists, pp. 24-25, 1989.

7. Johnson, Nicholas L., "Preliminary Analysis of the Fragmentation of the Spot 1 Ariane Third Stage," from "Orbital Debris From Upper-Stage Breakup," ed. Joseph P. Loftus, Jr., Progress in Astronautics and Aeronautics, v. 121, pp. 41-149, 1989.

8. Kessler, Donald, J., private communication, January 24th, 1991.

9. Ramohalli, Kumar et al., "Autonomous Space Processor for Orbital Debris: Final Report," submitted to USRA Summer Conference , Huntsville, Alabama, June 27-29 1989.

10. "Final Design for a Comprehensive Orbital Debris Management Program," University of Texas, May 4th 1990.

11. Petro, Andrew J., and Talent, David L., "Removal of Orbital Debris", from " Orbital Debris From Upper-Stage Breakup," ed. Joseph P. Loftus, Jr., Progress in Astronautics and Aeronautics, v. 121, pp.169-180, 1989.

12. "User's Guide to the Orbital Maneuvering Vehicle," National Aeronautics and Space Administration, Marshall Space Flight Center, 1987.

13. "User's Guide to the Orbital Maneuvering Vehicle," National Aeronautics and Space Administration, Marshall Space Flight Center, 1988.

14. Grumman Space Systems Division, "Tumbling Satellite Retrieval Kit Final Design Document," Grumman Corporation, Bethpage, NY, NASA Contract NAS 8-36641, November 1988.

15. Grumman Space Systems Division, "Concept Evaluation/Test for the Tumbling Satellite Retrieval Kit," Grumman Corporation, Bethpage, NY, NASA Contract NAS 8-36641, Part 1, October 1988.

16. McConnell, J. et al, "Concept Evaluation/Test for the Tumbling Satellite Retrieval (TSR) Kit," Grumman Corporation, Bethpage, NY, NASA Contract NAS 8-36641 (Data Requirement DR-08), October 1988.

7. Cable, D. A. et al, "Concept Definition Study for Recovery of Tumbling Satellites," Vol. 1, Executive Summary, Martin Marietta, Denver Aerospace Division, Contractor MCR-86-1329, (NASA Contract NAS8-36609), June 1986.

18. NASA Office of Public Affairs, Satellite Situation Report, Vol. 27, No. 4, NASA Goddard Spaceflight Center, Greenbelt Md, 1991.

19. King-Helle, D. G. et al, The RAE Table of Earth Satellites (1957-1986), Stockton Press, New York, 1987.

20. Johnson, Nicholas L., The Soviet Year in Space 1988, Teledyne Brown Engineering, Colorado Springs, Colorado, pp. 12-13, 1989.

21. Cochran, James, Auburn University, Private Communication, April 4th, 1991.

22. Turner, James, Private Communication, Feb. 12th, 1991.

23. Orthwein, William C., Clutches and Brakes: Design and Selection, Marcel Dekker, Inc., New York, p. 126, 1986.

24. Shigley, Joseph Edward & Mischke, Charles R., Mechanical Engineering Design, McGraw-Hill, New York, p. 650, 1989.

25. Chowdarry, Mahesh, "Thermal Compatibility Analysis of Passive Damping Treatment Proposed for Space Shuttle Remote Manipulator System," Masters Thesis, Old Dominion University, May 1991.

26. Bate, Roger R., Fundamentals of Astrodynamics, Dover Publications, New York, p.62, 1971.

27. Duncan, Robert C., Dynamics of Atmospheric Entry, McGraw-Hill New York, pp. 196-200, 1962.

28. Regan, Frank J., Reentry Vehicle Dynamics, AIAA Education Series, New York, p.110, 1984.

29. Mitchell, Terry R., "Shuttle-C: A Shuttle Derived Launch Vehicle," Twenty-Fifth Space Congress Proceedings, Cocoa Beach, Florida. April 26-29, pp. 12.1-12.4, 1988.

30. "Proximity Operations Analysis: Retrieval of the Solar Maximum Mission Observatory," National Aeronautics and Space Administration, Johnson Space Center, p. 15, April 1980.

APPENDIX A

APPENDIX A
TARGET SELECTION INFORMATION
SPACE OBJECT BOX SCORE

COSMOS PROGRAM CONTRIBUTION TO SPACE DEBRIS

NUMBER OF COSMOS SATELLITES IN ORBIT (ACTIVE AND INACTIVE)	886	
NUMBER OF COSMOS ROCKET BODIES	363	
NUMBER OF FRAGMENTS RESULTING FROM COSMOS PROGRAMS	2268+	*
TOTAL	3517+	

BREAKDOWN OF COSMOS ROCKET BODIES IN ORBIT

COMPLETELY INTACT COSMOS ROCKET BODIES IN LEO	219
NUMBER OF COSMOS C-1 SECOND STAGES	197
NUMBER OF COSMOS C-1 SECOND STAGES AT 89.2 INCLINATION	58

SOURCE: ROYAL AIRCRAFT ESTABLISMENT TABLES OF EARTH SATELLITES, SATELLITE SITUATION REPORT DECEMBER 1990 EDITION, AND THE SOVIET YEAR IN SPACE; 1987 & 1988 EDITIONS

* THERE IS AN ADDITIONAL NUMBER OF FRAGMENTS SMALLER THAN 4 cm ACROSS THAT WOULD NOT BE DETECTED BY CURRENT SENSORS.

APPENDIX B

TABLE B
COSMOS ROCKET BODIES
AT 82.9 DEG INCLINATION

COSMOS NUMBER	PERIOD (MINUTES)	APOGEE(KM)	PERIGEE(KM)
586	104.6	993	957
689	104.8	1010	960
700	104.5	980	959
755	104.7	994	964
807	103.0	1422	374
864	104.6	994	954
887	104.5	995	948
894	104.7	993	967
911	104.5	995	949
926	104.8	1003	970
962	104.6	1000	952
963	109.1	1200	1169
971	104.7	996	965
985	104.5	1006	935
994	104.7	995	967
996	104.5	996	944
1000	104.6	994	954
1027	104.5	986	959
1072	104.7	1010	949
1091	104.6	992	963
1092	104.6	997	955
1104	104.6	991	957
1150	104.7	997	962
1153	104.7	1009	952
1225	104.6	1010	941
1226	104.6	997	955
1295	104.5	996	945
1304	103.7	965	902
1308	104.6	994	959
1339	104.6	1008	940
1344	104.7	1010	950
1349	104.7	1000	959
1383	105.1	1028	969
1447	104.6	998	955
1464	104.7	999	958
1506	104.5	999	946
1513	104.6	1011	939
1531	104.8	1002	968
1553	104.6	997	954
1598	104.8	1000	966
1605	104.6	1008	946
1610	104.7	1003	955
1627	104.7	1014	953

TABLE B (CONT)
COSMOS ROCKET BODIES
AT 82.9 DEG INCLINATION

COSMOS NUMBER	PERIOD (MINUTES)	APOGEE(KM)	PERIGEE(KM)
1634	104.6	992	961
1655	104.9	1009	970
1704	104.6	995	955
1709	104.6	1001	952
1725	104.6	992	962
1727	104.7	1005	955
1759	104.6	1025	924
1816	104.7	1006	947
1821	104.9	1009	946
1861	104.7	991	964
1864	104.6	1001	951
1891	104.9	1023	934
1904	104.7	998	960
1934	104.5	994	947
1959	104.6	998	949

,,,,,,

,,,,,, *SOURCE: SATELLITE SITUATION REPORT, DECEMBER 1990 EDITION*

APPENDIX C

Appendix C
Rocket Body Moment of Inertia Calculations

Base Units:

$kg \equiv 1m$ $\quad m \equiv 1L$ $\quad sec \equiv 1T$

Derived Units:

$cm \equiv \frac{m}{100}$ $\quad N \equiv kg \cdot \frac{m}{sec^2}$ $\quad i \equiv 0..2$

$in \equiv 2.54 \cdot cm$ $\quad min \equiv 60 \cdot sec$ $\quad lb \equiv 4.448 \cdot N$

$rad \equiv 1$ $\quad J \equiv N \cdot m$ $\quad ft \equiv 12 \cdot in$

$rev \equiv 2 \cdot \pi \cdot rad$ $\quad kJ \equiv 1000 \cdot J$ $\quad Watt \equiv \frac{J}{sec}$

Nomenclature

mT	total mass of the rocket body
mt	mass of the fuel cylinder top
mc	mass of the fuel cylinder
mT1	mass of thruster mechanism
mT2	mass of nozzle
l	overall length of rocket body
t	thickness of top of fuel cylinder
lf	length of fuel section
lt	length of thruster mechanism
ln	length of nozzle
R	outside body radius
Rs	inside radius of cylinder
RT	outside radius of nozzle
RTi	inside radius of nozzle
dT	rotational stop time limit

$It = 922.0265\ kg\ m^2$ $IT1 = 2.868\ 10^3\ kg\ m^2$

$Ic = 5.755 \cdot 10^3 \cdot kg \cdot m^2$ $IT2 = 1.198 \cdot 10^3 \cdot kg \cdot m^2$

$I \equiv It + Ic + IT1 + IT2$ $I = 1.0743 \cdot 10^4\ kg \cdot m^2$

Angular energy in rocket body:

$\omega_0 \equiv 7 \cdot \frac{rev}{min}$ $\omega_1 \equiv 20 \cdot \frac{rev}{min}$ $\omega_2 \equiv 50 \cdot \frac{rev}{min}$

$E_i \equiv \frac{1}{2} \cdot I \cdot \omega_i^2$ $E = \begin{bmatrix} 2.8863 \\ 23.5619 \\ 147.262 \end{bmatrix} \cdot kJ$

work required to stop rotation:

$W_i \equiv \frac{E_i}{dT}$ $W = \begin{bmatrix} 9.6211 \\ 78.5397 \\ 490.8732 \end{bmatrix} \cdot Watt$

Required torque to stop angular motion of the rocket body idT = 5·min

$T_i \equiv I \cdot \frac{\omega_i}{dT}$ $T = \begin{bmatrix} 26.25 \\ 74.9999 \\ 187.4998 \end{bmatrix} \cdot N \cdot m$

Equations are from Mechanical Engineering Design, fifth edition, by Joseph Shigley & Charles Mischke. McGraw-Hill, New York. pp 549-561

Vehicle physical model dimensions

$ml \equiv 2200\ kg$ $l \equiv 7.5 \cdot m$ $R \equiv 1.2\ m$

$mt \equiv 50\ kg$ $t \equiv 2\ in$ $Rs \equiv 1.2\ m - t$

$mc \equiv 1000\ kg$ $lf \equiv 5\ m$ $RT \equiv 0.7\ m$

$mT1 \equiv 1000\ kg$ $lt \equiv 1.5\ m$ $RTi \equiv RT - 2 \cdot t$

$mT2 \equiv 150\ kg$ $ln \equiv 1 \cdot m$ $dT \equiv 5\ min$

Center of mass (CM): d is distance from CM to intersection of fuel section and thruster section.

$$d \equiv \frac{mt\left[\frac{t}{2} + lf\right] + mc\cdot\frac{lf}{2} - mT1\cdot\frac{lt}{2} - mT2\cdot\left[\frac{ln}{2} + lt\right]}{mT} \qquad d = 0.7733\cdot m$$

Mass moment of inertia analysis:

$$It \equiv \frac{mt}{12}\left[3\cdot R^2 + t^2\right] + mt\cdot\left[\frac{t}{2} + lf - d\right]^2$$ fuel cylinder top

$$Ic \equiv \frac{mc}{12}\left[3\cdot R^2 + 3\cdot Rs^2 + lf^2\right] + mc\cdot\left[\frac{lf}{2} - d\right]^2$$ fuel cylinder

$$IT1 \equiv \frac{mT1}{12}\left[3\cdot R^2 + lt^2\right] + mT1\left[\frac{lt}{2} + d\right]^2$$ thruster mechanism

$$IT2 \equiv \frac{mT2}{12}\left[3\,RT^2 + 3\cdot RTi^2 + ln^2\right] + mT2\cdot\left[\frac{ln}{2} + lt + d\right]^2$$ nozzle

ORIGINAL PAGE IS
OF POOR QUALITY

APPENDIX D

SAMPLE CALCULATIONS FOR BRAKE DATA

This section will provide clarification into how the brake data calculations were made for this report. Prior to making the calculations for torque required for stopping the spinning arms and energy that will need to be dissipated by the brake, some assumptions will need to be advanced. Important governing factors for both calculations are the spinning and non-spinning moments of inertia, see Figure D.1 for locations.

The spinning portions will include the captured rocket body and the OMV's arms, cradle, spin table and spin table shaft moments of inertia. The rocket body moment of inertia has been calculated in Appendix C. The moment of inertia for the arms and cradle for the current design has been calculated in Appendix C. The last portion of the spinning component's moment of inertia will come from the spin table. The spin table will be modeled after a 5 cm thick plate disk that is 3.965 m in diameter made of aluminum. While the actual thickness of the spin table is envisioned to be less than 5 cm, using this large value will compensate for some components (actuators, supports, sensors, and joints) not included directly in the calculations.

A similar approach was taken in modeling the non-spinning portions of the design. The OMV was assumed to be a solid cylinder 14' 8" in diameter and 71" in height of constant density for moment of inertia calculation purposes. The base plate of the ODC was

considered to have the same diameter as the OMV and be made of aluminum 5 cm thick. The extra thickness in the base plate will compensate for structural supports, OMV-ODC interfaces, on board computers, and motor supports not included directly in the calculations. The spin table shaft, motor, brakes, and coupling were assumed to have negligible moments of inertia compared to the other portions of the system and were dropped from the calculations.

Symbols Used In Sample Calculations

E	Heat Energy of friction produced by brakes
F_f	Force acting on each brake shoe
I_1	Moment of Inertia for spinning section of RBRV + C-1B
I_2	Moment of Inertia for non-spinning section of RBRV
n	Number of brake pads
p_{dia}	Diaphragm Pressure
p_{max}	Maximum Design Pressure of the brake material
r	Radial distance from center line of shaft to brake pads
r_{dia}	Radial distance from center line of shaft to diaphragm inner diameter
T	Torque applied by the brakes
t_s	Stopping Time
w	Width of Brakes
ω_1	Angular Velocity of rotating section of RBRV
ω_2	Angular Velocity of non-rotating section of RBRV
μ	Coefficient of Friction

The moments of inertia for the separate sections was shown to be as follows:

Section	Portion	Inertia Kg m²
Moving	Rocket Body	10743
	ODC (Spin Table)	4541
	TOTAL I_1	15284
Non-moving	OMV	25298
	ODC (Base Plate)	5452
	TOTAL I_t	30750

The rocket body rotational velocity upper limit was set at 50 RPM and will form the basis of these calculations. Since some lighting will be provided by the sun and limitation on relay satellite coverage will allow for only a thirty minute capture window, the braking portion of the mission should be kept to a five minutes or less.

The stopping torque will be:

$$T=\frac{I_1 I_2(\omega_1-\omega_2)}{t_1(I_1+I_2)}$$

$$T=\frac{15284 Kg\,m^2 * 30750 Kg\,m^2 (50\ RPM-0)}{300\ \sec(15284 Kg\,m^2+30750 Kg\,m^2)}$$

$$T = 28.36\ N\ m$$

The heat energy resulting from friction which will have to be dissipated from the brake can be found by:

$$E = \frac{I_1 I_2 (\omega_1 - \omega_2)^2}{2(I_1 + I_2)}$$

$$E = \frac{15284 Kg\,m^2 * 30750 Kg\,m^2 (50\,RPM - 0)^2}{2(15284 Kg\,m^2 + 30750 Kg\,m^2)}$$

$$E = 3544\ J[45]$$

These values are not excessive and will not prove to be a major design burden. This can be seen in the next series of calculations which will cover the brakes themselves.

For these calculation, a pneumatically operated system was envisioned to consist of two externally mounted brake pads of molded asbestos blocks. Figure D.2 provides a diagram of the brake layout. There will be the need for a gap between the two pads of ~10 degrees, which allows each pad to have a ~170 degree contact area. To prevent damage to an aluminum spin table shaft, a steel collar will be installed on the shaft to provide the braking surface. This collar was assumed to be 8 cm in outer diameter and bored to suit the shaft diameter. A median value of .35 was chosen for the coefficient of friction between these materials. The median maximum pressure value of 675 kPa was chosen for molded asbestos blocks. The brake width, braking force and diaphragm pressure could be determined once these assumptions and constraints applied.

The brake width (w) relationship is:

$$w = \frac{T/n}{2 \mu p_{MAX} r^2 \sin(\phi/2)}$$

$$w = \frac{28.35Nm/2}{2\,(.35)\,(675kPa)\,.04^2 \sin(2.967/2)}$$

$$w = 1.882 \text{ cm}$$

It should be noticed that this equation is very sensitive to the collar radius. Next, the force needed to be applied to each shoe may be determined:

$$F_s = \frac{P_{MAX}}{2} r\, w\,(\phi + \sin\phi)$$

$$F_s = \frac{675kPa}{2}\,(.04m)\,(.0188)\,(2.967 + \sin 2.967)$$

$$F_s = 798.302 \text{ N}$$

If three cm are allowed for the pad thickness, diaphragm retainer and bonding, the pressure on the diaphragm can be determined by:

$$p_{DIA} = \frac{F_s}{\pi\, r_{eff}^2}$$

$$p_{DIA} = \frac{798.3N}{\pi\, .06^2}$$

$$p_{DIA} = 31731 \text{ Pa.}$$

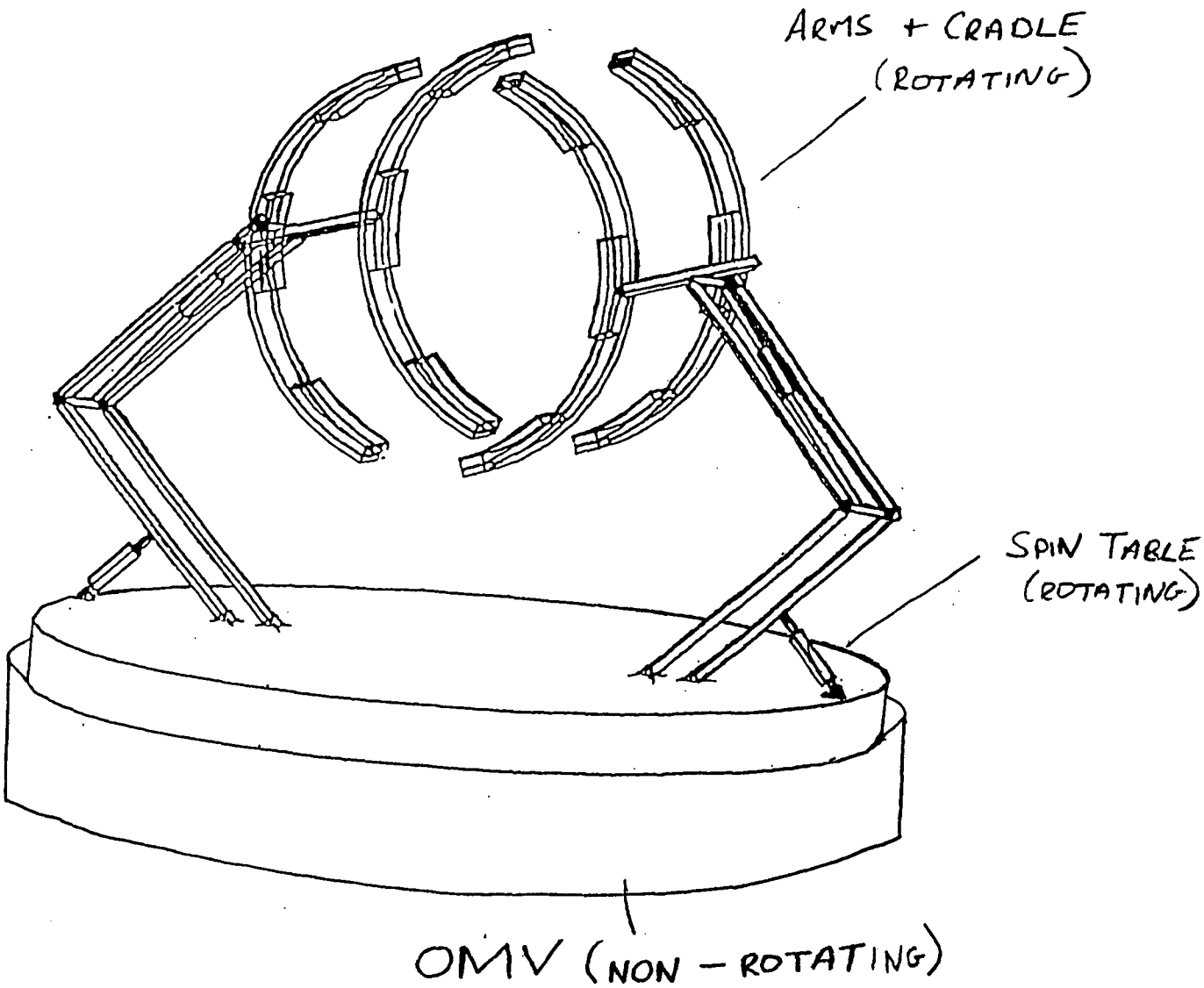

Figure D1 - Distribution of Inertia

APPENDIX E

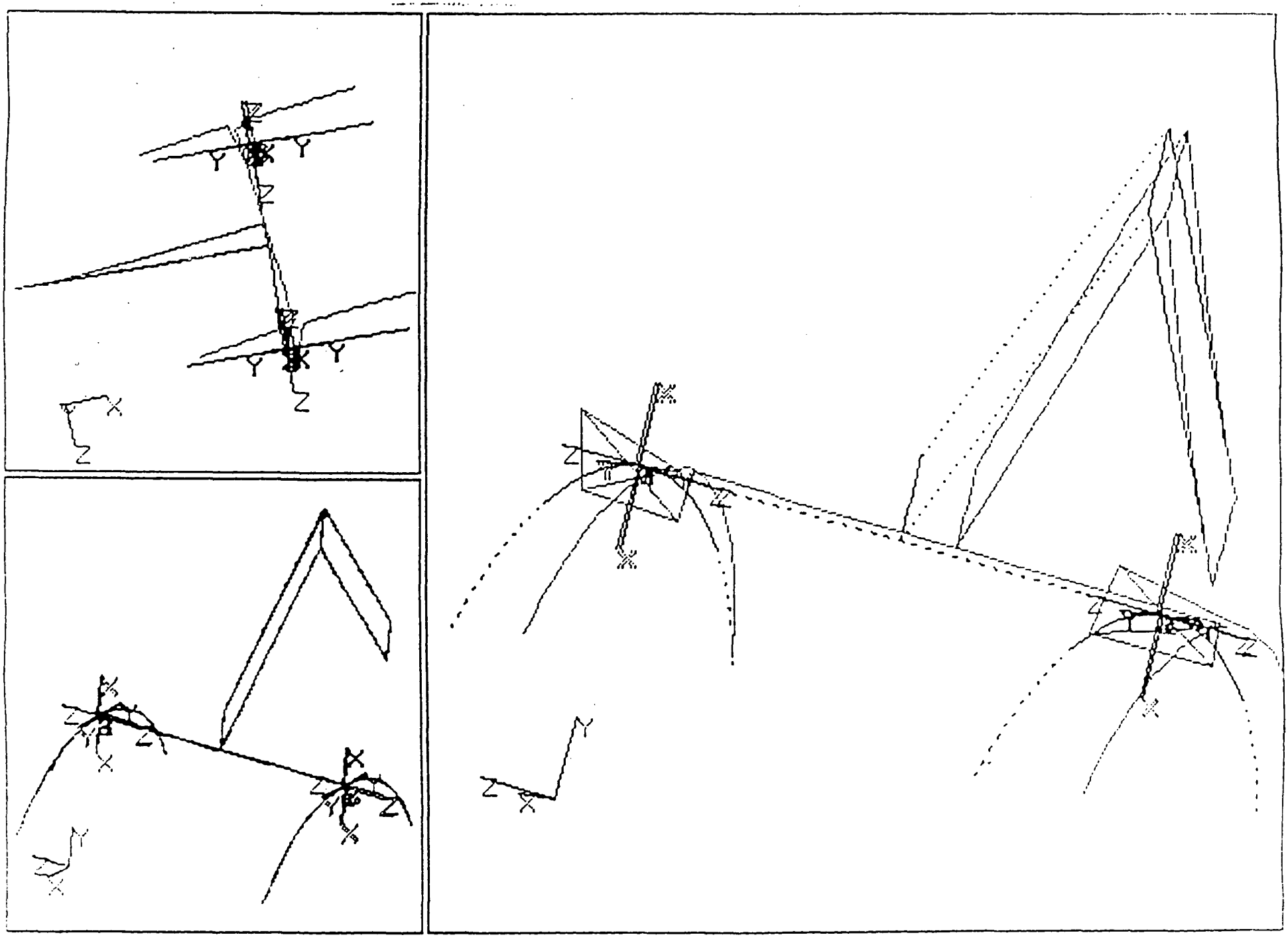

PATRAN output file of Deformation from Applied Torque

APPENDIX F

Position Analysis of Arms

****

Given

$l1 \equiv 1.71$ m

$l2 \equiv 1.71$ m

$H \equiv 2.42$ m

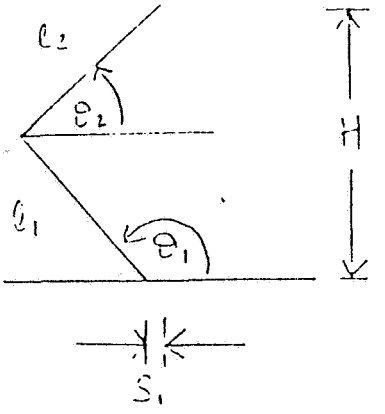

$\theta1 := 3\cdot\frac{\pi}{4}$ $\quad \theta2 := \frac{\pi}{4}$ $\quad s1 \equiv 0$

Given

$l1\cdot\sin(\theta1) + l2\cdot\sin(\theta2) - H \approx 0$

$l1\cdot\cos(\theta1) + l2\cdot\cos(\theta2) - s1 \approx 0$

$$\text{find}(\theta1,\theta2) = \begin{bmatrix}2.355\\0.786\end{bmatrix}$$

$\theta1 := 3\cdot\frac{\pi}{4}$ $\quad \theta2 := \frac{\pi}{4}$ $\quad s2 \equiv -1.21$

Given

$l1\cdot\sin(\theta1) + l2\cdot\sin(\theta2) - H \approx 0$

$l1\cdot\cos(\theta1) + l2\cdot\cos(\theta2) - s2 \approx 0$

$$\text{find}(\theta1,\theta2) = \begin{bmatrix}2.693\\1.376\end{bmatrix}$$

Therefore the ranges are as follows: $2.693 < \theta1 < 3\pi/4$

$1.376 < \theta2 < \pi/4$

Given

$d1 \equiv .4 \quad m$

$C1 \equiv 1 \quad m$

$i := 0 \,..\, 1$

$$\theta 1_i := \left[3 \cdot \frac{\pi}{4} - 2.693\right] \cdot i + 2.693$$

$$\phi_i := \operatorname{atan}\left[d1 \cdot \frac{\sin\left[\theta 1_i\right]}{C1 + d1 \cdot \cos\left[\theta 1_i\right]}\right]$$

$$a1_i := d1 \cdot \frac{\sin\left[\theta 1_i\right]}{\sin\left[\phi_i\right]}$$

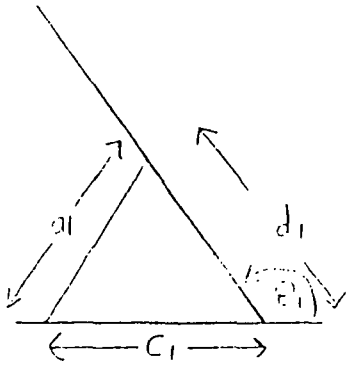

i	θ1	φ	a1
	i	i	i
0	2.693	0.265	0.663
1	2.356	0.376	0.771

The ranges of the length of actuator arm 1, required to give the desired angles, are: .663 m < a1 < .771 m

Position Analysis of Upper Arm Actuator System
****

Given

$$\theta 2_i := \left[\frac{\pi}{4} - 1.376\right] \cdot i + 1.376$$

$$\phi 2_i := \operatorname{atan}\left[12 \cdot \frac{\sin\left[\theta 2_i\right]}{12 \cdot \cos\left[\theta 2_i\right] + .2}\right]$$

$$a2_i := 12 \cdot \frac{\sin\left[\theta 2_i\right]}{\sin\left[\phi 2_i\right]}$$

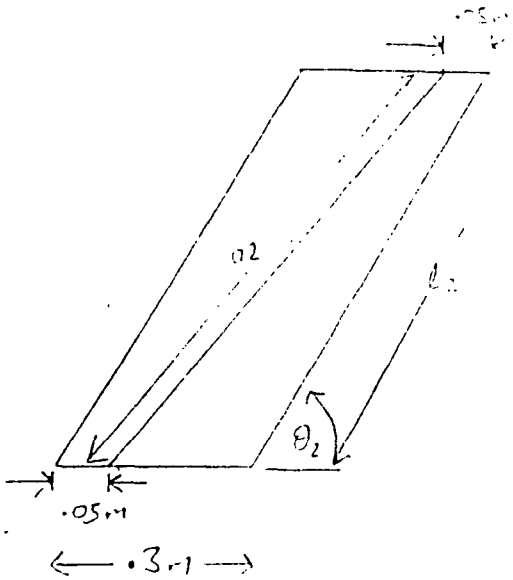

i	θ2	φ2	a2
	i	i	i
0	1.376	1.264	1.76
1	0.785	0.709	1.357

The actuator length variations required for the desired variations in θ2 are: 1.76 m < a2 < 1.357 m

Velocity Analysis for Arms

****

NOTE: in the following computations a derivative with respect to time is denoted with a "d" preceding the variable

This section of the analysis attempts to obtain the required angular velocities necessary to achieve an approach velocity of 1 m/sec.

Given

$d\theta 1_0 \equiv -.00015$ rad/second $\qquad d\theta 1_1 \equiv -.0006$ rad/second

By constraining the arms to keep H constant:

$$d\theta 2_i := \frac{-\left[d\theta 1_i \cdot l1 \cdot \cos\left[\theta 1_i\right]\right]}{l2 \cdot \cos\left[\theta 2_i\right]}$$

$$ds_i := -\left[l2 \cdot \sin\left[\theta 2_i\right] \cdot d\theta 2_i + l1 \cdot \sin\left[\theta 1_i\right] \cdot d\theta 1_i\right]$$

$d\theta 1_i$	$d\theta 2_i$	ds_i
$-1.5 \cdot 10^{-4}$	$-6.983 \cdot 10^{-4}$	0.001
$-6 \cdot 10^{-4}$	$-6 \cdot 10^{-4}$	0.001

These values of θ1 & θ2 are the target values to be reached by the actuator extensions at these particular angles

Velocity Analysis of Lower Arm Actuator System

****

This section of analysis attempts to obtain required actuator velocities necessary to impart the above target angular velocities

Given

$da1a := .00003928$ m/s At initial position of θ1 = 2.693 radians

$$J1a := \begin{bmatrix} -a1 \cdot \sin\left[\phi_0\right] & d1 \cdot \sin\left[\theta 1_0\right] \\ a1 \cdot \cos\left[\phi_0\right] & -d1 \cdot \cos\left[\theta 1_0\right] \end{bmatrix}$$

$$B1a := \begin{bmatrix} -\cos\left[\phi_0\right] \\ -\sin\left[\phi_0\right] \end{bmatrix}$$

$$\begin{bmatrix} d\phi a \\ d\Theta 1a \end{bmatrix} := (J1a)^{-1} \cdot B1a \cdot da1a$$

$$\begin{bmatrix} d\phi a \\ d\Theta 1a \end{bmatrix} = \begin{bmatrix} 6.848 \cdot 10^{-5} \\ -1.5 \cdot 10^{-4} \end{bmatrix}$$

Velocity analysis at $\Theta 1 = 3\pi/4$

da1b := .00022015

$$J1b := \begin{bmatrix} -a1 \cdot \sin(\phi_1) & d1 \cdot \sin(\Theta 1_1) \\ a1 \cdot \cos(\phi_1) & -d1 \cdot \cos(\Theta 1_1) \end{bmatrix}$$

$$B1b := \begin{bmatrix} -\cos(\phi_1) \\ -\sin(\phi_1) \end{bmatrix}$$

$$\begin{bmatrix} d\phi b \\ d\Theta 1b \end{bmatrix} := (J1b)^{-1} \cdot B1b \cdot da1b$$

$$\begin{bmatrix} d\phi b \\ d\Theta 1b \end{bmatrix} = \begin{bmatrix} 1.24 \cdot 10^{-4} \\ -6 \cdot 10^{-4} \end{bmatrix}$$

The required actuator velocity to impart an angular velocity of -.0006 rad/s, is 2.2015 * 10^-4 m/s

Velocity Analysis of Upper Arm Actuator System

The two actuator velocities are obtained at the extremes of the range of $\Theta 2$ to maintain a ds velocity of 1 mm/sec.

The first analysis is at $\Theta 2$= 1.376, with a required angular velocity $\Theta 2$ of -6.983 * 10^-4 rad/s

da2a := .00012972 m/s

$$J2a := \begin{bmatrix} 12 \cdot \sin\left[\begin{matrix}\theta 2\\ 0\end{matrix}\right] & -a2 \cdot \sin\left[\begin{matrix}\phi 2\\ 0\end{matrix}\right] \\ -12 \cdot \cos\left[\begin{matrix}\theta 2\\ 0\end{matrix}\right] & a2 \cdot \cos\left[\begin{matrix}\phi 2\\ 0\end{matrix}\right] \end{bmatrix} \qquad B2a := \begin{bmatrix} -\cos\left[\begin{matrix}\phi 2\\ 0\end{matrix}\right] \\ -\sin\left[\begin{matrix}\theta 2\\ 0\end{matrix}\right] \end{bmatrix}$$

$$\begin{bmatrix} d\theta 2a \\ d\phi 2a \end{bmatrix} := (J2a)^{-1} \cdot B2a \cdot da2a$$

$$\begin{bmatrix} d\theta 2a \\ d\phi 2a \end{bmatrix} = \begin{bmatrix} -4 \\ -6.983 \cdot 10 \\ -4 \\ -6.749 \cdot 10 \end{bmatrix}$$

Required actuator velocity at this point to impart the appropriate angular velocity is 1.2972 * 10^-4 m/s

The second analysis is at $\theta 2 = \pi/4$, and the required $d\theta 2$ is -.0006 rad/sec

$da2b := .0000754 \ \ m/s$

$$J2b := \begin{bmatrix} 12 \cdot \sin\left[\begin{matrix}\theta 2\\ 1\end{matrix}\right] & -a2 \cdot \sin\left[\begin{matrix}\phi 2\\ 1\end{matrix}\right] \\ -12 \cdot \cos\left[\begin{matrix}\theta 2\\ 1\end{matrix}\right] & a2 \cdot \cos\left[\begin{matrix}\phi 2\\ 1\end{matrix}\right] \end{bmatrix}$$

$$B2b := \begin{bmatrix} -\cos\left[\begin{matrix}\phi 2\\ 1\end{matrix}\right] \\ -\sin\left[\begin{matrix}\theta 2\\ 1\end{matrix}\right] \end{bmatrix}$$

$$\begin{bmatrix} d\theta 2b \\ d\phi 2b \end{bmatrix} := (J2b)^{-1} \cdot B2b \cdot da2b$$

$$\begin{bmatrix} d\theta 2b \\ d\phi 2b \end{bmatrix} = \begin{bmatrix} -4 \\ -6 \cdot 10 \\ -4 \\ -5.527 \cdot 10 \end{bmatrix}$$

Therefore actuator # 2 must move at 7.54 * 10^-5 m/s to impart a $\theta 2$ motion of -6 * 10^-6 rad/s at this point

APPENDIX G

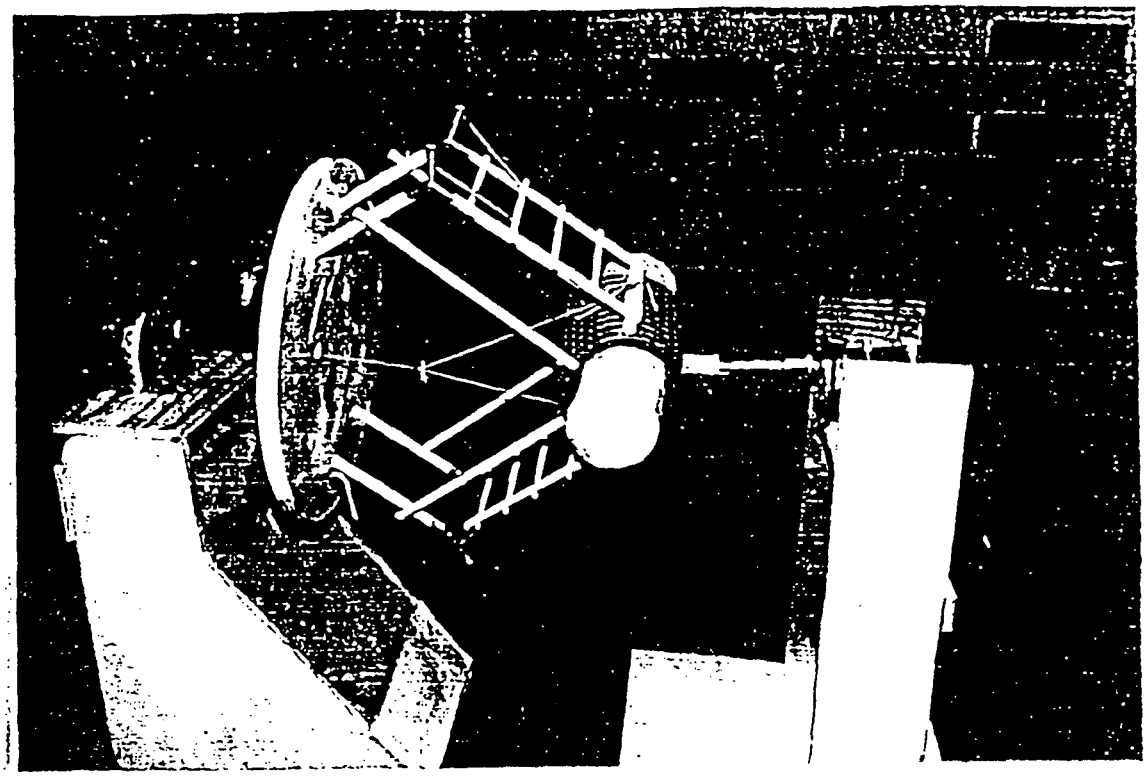

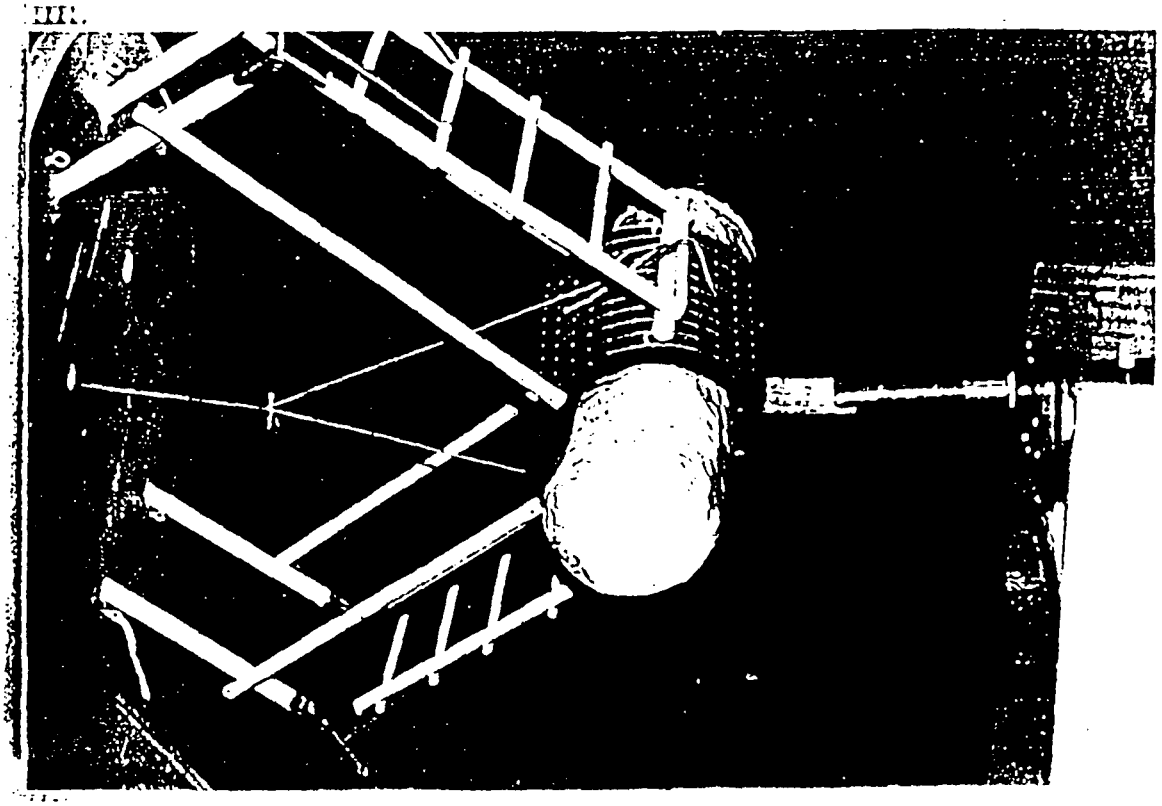

ORIGINAL PAGE IS
OF POOR QUALITY

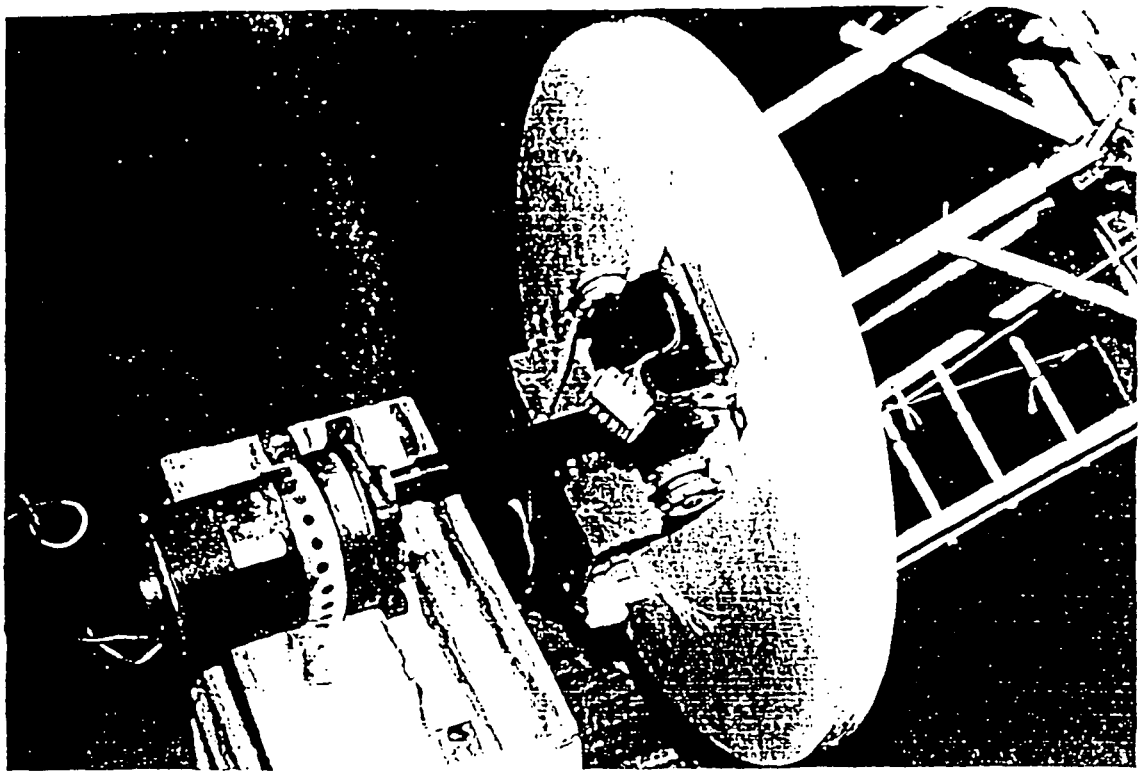

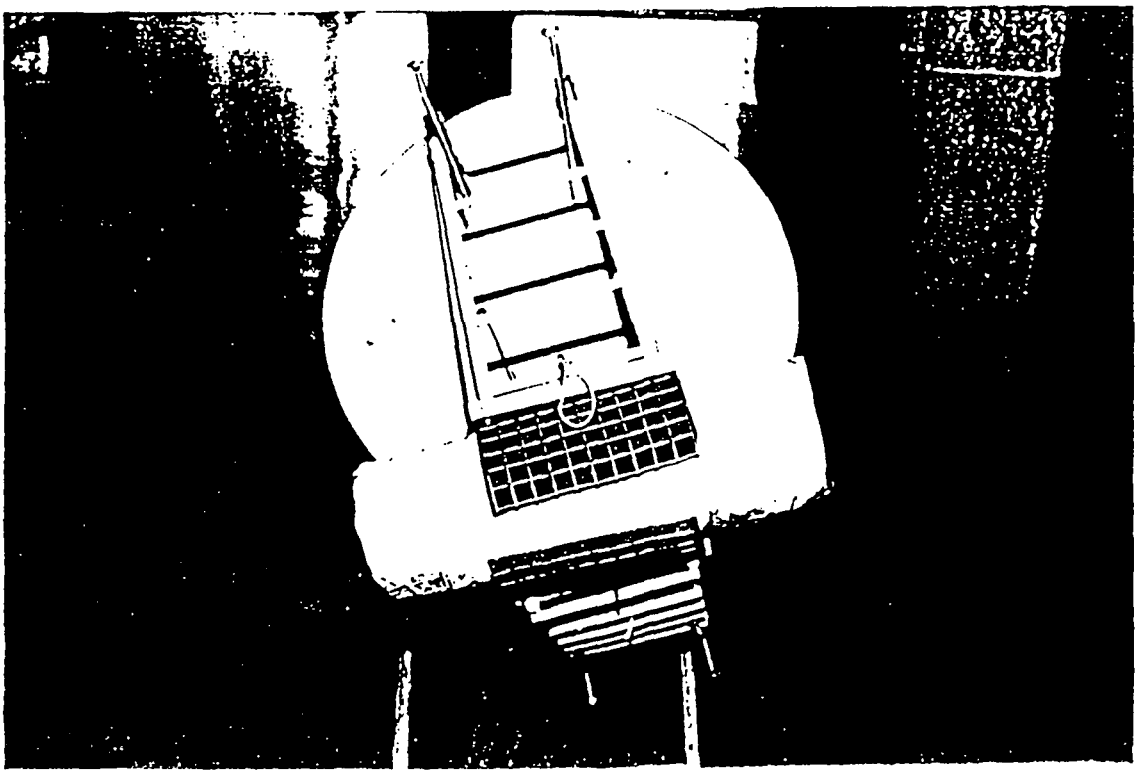

ORIGINAL PAGE IS
OF POOR QUALITY